This is a preprint of an article accepted for publication in Journal of Earthquake Spectra on 23 January 2015. The published article is available online at
http://earthquakespectra.org/doi/abs/10.1193/061414EQS086M?code=eeri-site
To be cited as: Daneshvar P., Bouaanani N., Goda K., Atkinson G. 2015. Damping reduction factors for crustal, inslab, and interface earthquakes characterizing seismic hazard in South-Western British Columbia, Canada. Journal of Earthquake Spectra, 32(1): 45–74.

Damping Reduction Factors for Crustal, Inslab, and Interface Earthquakes Characterizing Seismic Hazard in South-Western British Columbia, Canada

Poulad Daneshvar,[a] M.EERI, Najib Bouaanani,[b] M.EERI, Katsuichiro Goda,[c] M.EERI and Gail M. Atkinson,[d] M.EERI

High-damping displacement spectra and corresponding damping reduction factors (η) are important ingredients for seismic design and analysis of structures equipped with seismic protection systems, as well as for displacement-based design methodologies. In this paper, we investigate η factors for three types of earthquakes characterizing seismic hazard in south-western British Columbia, Canada: (i) shallow crustal, (ii) deep inslab, and (iii) interface subduction earthquakes. We use a large and comprehensive database including records from recent relevant earthquakes, such as the 2011 Tohoku event. Our key observations are: (i) there is negligible dependence of η on soil class; (ii) there is significant dependence of η on the frequency content and duration of ground motions that characterize the different record types and (iii) η is dependent on period, particularly for inslab events. Period-dependent equations are proposed to predict η for damping ratios between 5% and 30% corresponding to the three event types.

INTRODUCTION

Elastic displacement spectra associated with damping levels higher than the conventional 5% critical damping are important in the seismic design and evaluation of structures equipped with energy dissipating and seismic isolation systems. High-damping displacement spectra are also required for displacement-based design and evaluation techniques, such as the Direct Displacement-Based Design method (Priestley and Kowalsky 2000; Priestley et al. 2007). Such displacement spectra can be determined using: (i) ground motion prediction equations

[a] Ph.D. Candidate, Department of Civil, Geological and Mining Engineering, Polytechnique Montréal, Montréal, QC H3C 3A7, Canada.
[b] Professor, Department of Civil, Geological and Mining Engineering, Polytechnique Montréal, Montréal, QC H3C 3A7, Canada. Corresponding author. E-mail: najib.bouaanani@polymtl.ca
[c] Senior Lecturer, Department of Civil Engineering, University of Bristol, Bristol, BS8 1T8, UK.
[d] Professor, Department of Earth Sciences, Western University, London, ON N6A 3K7, Canada.

(GMPEs) developed specifically for damping levels higher than 5%, or (ii) damping reduction factors, denoted hereafter by η, which are defined as the ratio between the 5%-damped displacement spectrum $S_d(T,5\%)$ and displacement spectra $S_d(T,\xi)$ for higher damping levels ξ at a period T

$$\eta(T,\xi) = \frac{S_d(T,\xi)}{S_d(T,5\%)} \quad (1)$$

A number of GMPEs predicting spectral amplitudes at various damping levels have been proposed for different regions, e.g. Chen and Yu (2008) for western North America (WNA), and Akkar and Bommer (2007) and Cauzzi and Faccioli (2008) for Europe. These are useful in conducting probabilistic seismic hazard analysis to assess seismic hazard values for higher damping ratios. On the other hand, most guidelines and building codes adopt the approach of damping reduction factors (e.g. UBC-97, Eurocode8 2004, CHBDC 2006, ATC 2010, AASHTO 2010, and ASCE7-10). An advantage of the latter approach is that these damping reduction factors can be applied directly to code-prescribed spectral amplitudes to evaluate damping effects.

The main objectives of this work are: (i) to determine and characterize damping reduction factors corresponding to three event types contributing to seismic hazard in south-western British Columbia (BC), i.e. crustal, inslab, and interface events, and (ii) to propose model equations for the median of these damping reduction factors as a function of damping ratio, period, and soil class. The adopted procedure for developing such damping reduction factors for Vancouver is based on the evaluation of the damping reduction factors using various sets of ground motion records that are selected based on seismic deaggregation (i.e. dominant scenarios). The parameterization of the prediction models for η is guided by the current seismic provisions in Canada (NBCC 2010). This provides a practical means to extend the usability of the current seismic design requirements in place. Vancouver is selected to conduct probabilistic seismic hazard analysis (PSHA); site conditions corresponding to soft rock and soft soil sites, which characterize the Greater Vancouver region, are considered.

Various equations have been proposed in the literature to approximate damping reduction factors considering seismic hazard in different regions. Newmark and Hall (1973, 1982) used the horizontal and vertical components of 14 pre-1973 California ground motions to propose damping reduction factors corresponding to damping levels lower than 20%. Bommer et al. (2000) studied the damped displacement spectra of 183 ground motion components from 43 shallow earthquakes recorded on rock, stiff and soft soil sites in Europe and the Middle East. They proposed an equation which was implemented in Eurocode 8 (2004). The Chinese guidelines for seismically isolated structures include a period-independent equation for damping reduction factors (Zhou et al. 2003). Lin and Chang (2004) studied 1037 accelerograms recorded in the United States to propose period-dependent damping reduction factors for periods between 0.1 s and 6 s and damping ratios between 2% and 50%. Atkinson and Pierre (2004) extended the simulations performed to generate a dataset of synthetic records which was used in developing the GMPE of Atkinson and Boore (1995) for scenarios between **M**4.0 and **M**7.25 at hypocentral distances of 10 km to 500 km. The 1%, 2% 3%, 5%, 7%, 10%, and 15%-damped response spectra were computed and finally a magnitude-distance independent set of η factors was proposed for periods between 0.05 s and 2 s, magnitudes greater than 5, and distances shorter than 150 km. Cameron and Green (2007) proposed a set of damping modification factors for damping levels between 1% and 50% for magnitude-binned ground motion records from shallow crustal events. Ground motion duration was shown

to be highly influential on damping reduction factors, whereas source-to-site distance was found to have negligible effect for damping levels of 2% and above. They also showed that site conditions have minor influence on damping modification factors for shallow crustal events in active tectonic regions. AASHTO (2010) includes a simplified equation to obtain damping reduction factors for damping levels up to 50%, while suggesting caution regarding its use for damping ratios greater than 30%. Rezaeian et al. (2014) studied a database of 2250 records from shallow crustal ground motions and developed a magnitude- and distance-based model to predict damping modification factors for the average horizontal component of ground motion and damping levels of between 0.5% and 30%. They observed the period dependency of the damping modification factors and also reported a strong dependency of these factors on ground motion duration. The abovementioned factors and equations are all period-independent, except for those proposed by Atkinson and Pierre (2004), Lin and Chang (2004), Cameron and Green (2007) and Rezaeian et al. (2014). A recent investigation of several period-dependent and period-independent damping reduction factors by Cardone et al. (2009) showed that period-dependent models provide the most accurate predictions of computed displacement spectra. Furthermore, Bradley (2014) reiterates the period- and duration-dependency of damping reduction factors while questioning the accuracy of a number of proposed equations, namely the one prescribed by Eurocode 8 (2004) where response amplification is characterized in terms of source- and site-specific effects. It should be noted that some older equations are based on studies that may lack adequate record processing of the used accelerograms (i.e. such as filtering and zero-padding) and therefore might not be suitable for long period ranges.

An important consideration is that the majority of the previous studies have focused upon ground motions for shallow crustal earthquakes, whereas ground motions for subduction earthquakes (including deep inslab and mega-thrust interface events) have not been much investigated. The large magnitudes of mega-thrust subduction earthquakes, and the potentially-high stress drops for deep inslab earthquakes, are important factors that control the duration and frequency content of ground motions - which are relevant properties for damped structural responses. It is therefore expected that the differing characteristics of ground motions for different earthquake types that contribute to hazard have major influence on the damping reduction factors. This is a research gap in the current literature that warrants further investigations, and is the focus of this study.

Southwestern BC is a seismically-active region with three distinct event types that contribute to seismic hazard: (i) shallow crustal, (ii) deep inslab, and (iii) interface Cascadia subduction earthquakes. Ground motions recorded in environments similar to these three tectonic settings have been shown to have distinctive characteristics in terms of frequency content and duration (Pina 2010; Jayaram et al. 2011; Tehrani et al. 2014). It is not known whether damping reduction factors corresponding to the three event types would be different, as there are no recent studies that address these effects. This is the novelty of this study. There are several highly-populated urban centers in BC, such as the Greater Vancouver region, where major infrastructure was constructed prior to the adoption of modern seismic provisions in the mid-1970s. The rehabilitation of this infrastructure using seismic isolation or added damping requires the availability of appropriate damping reduction factors. Such damping reduction factors are also required for displacement-based design of new infrastructure in the region. To the authors' knowledge however, there is no published work that investigated and compared damping reduction factors corresponding to crustal, inslab, and interface earthquakes characterizing seismic hazard in south-western BC or a similar tectonic setting.

PRELIMINARY SELECTION OF GROUND MOTION RECORDS

The records used in this study are selected from two sources: (i) the PEER-NGA database to represent worldwide shallow crustal events, and (ii) K-NET, KiK-net and SK-net databases to represent inslab and interface events. The record characteristics of the PEER-NGA database can be found at http://peer.berkeley.edu/nga/index.html, while those of K-NET, KiK-net and SK-net databases are available at www.k-net.bosai.go.jp, www.kik.bosai.go.jp and www.sknet.eri.u-tokyo.ac.jp, respectively. Further information about the Japanese databases can be found in Goda and Atkinson (2009) and Goda and Atkinson (2010).

The following selection criteria were applied to form a preliminary combined dataset of K-NET, KiK-net and SK-net records enriched with earthquakes that occurred up to 2012: (1) maximum depth is 500 km; (2) minimum Japan Meteorological Agency (JMA) magnitude is 3.0; (3) maximum hypocentral distance is 1500 km; (4) minimum horizontal peak ground acceleration (PGA, geometric mean) is 1.0 cm/s^2; and (5) at least 10 records are available for each seismic event satisfying the preceding four conditions. This preliminary selection led to a combined set of 555,750 records from 6261 earthquakes. To emphasize important characteristics of damaging ground motions in terms of amplitudes, spectral content, and duration, we further refined the PEER-NGA and the combined K-NET/KiK-net/SK-net dataset by applying additional selection criteria: (i) only horizontal components recorded on ground surface are considered; (ii) magnitude-distance cut-off limits considered by Goda and Atkinson (2009) are applied with the minimum moment magnitude **M** equal to 6.0; (iii) average shear-wave velocity in the uppermost 30 m V_{s30} between 180 m/s and 760 m/s representing soil classes C and D; and (iv) geometric means of the PGA and PGV of the two horizontal components greater than 100 cm/s^2 and 10 cm/s, respectively. These refined selection criteria resulted in a total of 2302 earthquake horizontal accelerograms. The number of accelerograms for crustal earthquakes is 1098 (716 components are from the NGA database while 382 components are from the combined Japanese database); the number of accelerograms for inslab earthquakes is 622; and the number of accelerograms for interface earthquakes is 582. The interface records are either from the **M**8.3 2003 Tokachi-oki or the **M**9.0 2011 Tohoku earthquakes to capture the record properties related to large magnitudes of the Cascadia subduction events.

RECORD SELECTION BASED ON PROBABILISTIC SEISMIC HAZARD ANALYSIS

The seismic hazard model developed by Atkinson and Goda (2011) for western Canada is adopted herein to conduct PSHA for Vancouver. This PSHA is based on simulated seismic activities spanning 5 million years, and an annual non-exceedance probability of 0.9996, i.e. a return period of 2500 years. It is carried out at different periods T^* = 0.2 s, 0.5 s, 1.0 s, 2.0 s, and 3.0 s to investigate the effect on high-damping spectral amplitudes. The deaggregation analysis is based on an "approximately equal criterion" as discussed by Hong and Goda (2006). Deaggregation results are shown in Table 1 in terms of mean moment magnitude **M** and mean rupture distance R_{rup} at each period T^* for each event type and soil class, in accordance with standard deaggregation practice. The identified scenarios are not overly sensitive to the choice of mean versus mode. Each of the three sets contains the deaggregation results for soil classes C and D. It can be seen that for crustal and inslab event types, deaggregation results are affected by the choice of T^* while they are almost insensitive to the changes in soil class. The deaggregation results for interface events are shown to be independent of both soil class and

period $T^* \leq 3$ s. The results in Table 1 suggest that a final selection of ground motions taking account of appropriate scenarios for each earthquake type should be conducted.

Table 1. Magnitude-distance criteria for the selected records based on deaggregation results

		T^* = 0.2 s		T^* = 0.5 s		T^* = 1.0 s		T^* = 2.0 s		T^* = 3.0 s	
Event Type	Soil Class	**M**	R_{rup}	**M**	R_{rup}	**M**	R_{rup}	**M**	R_{rup}	**M**	R_{rup}
Crustal	C	6.5	11	6.7	13	6.8	15	7.0	15	7.1	15
	D	6.5	14	6.7	14	6.8	18	7.0	15	7.1	17
Inslab	C	6.8	62	7.0	55	7.0	54	7.1	54	7.2	58
	D	6.9	61	7.0	56	7.0	52	7.1	51	7.2	53
Interface	C	8.6	141	8.6	141	8.6	142	8.6	142	8.6	141
	D	8.6	142	8.7	142	8.6	141	8.6	141	8.6	141

FINAL SELECTED RECORDS

The final step in the scenario-based record selection is to identify a set of records representing each event type and the corresponding mean **M** and mean R_{rup} obtained from deaggregation. For this purpose, a **M**-R_{rup} trade off of 40 km, 60 km, and 60 km is adopted for crustal, inslab, and interface events, respectively. This suggests that, for example, a crustal record having a magnitude of one unit lower than the mean **M** obtained from deaggregation, will be selected provided that it has a R_{rup} of 40 km shorter than the mean R_{rup} obtained from deaggregation (Baker and Cornell 2006). For inslab and interface records, a slightly longer trade-off distance of 60 km than crustal records is considered to account for a wider distance range of these records. For the inslab and interface datasets considered, the **M**-R_{rup} trade-off distance has a negligible effect on the selected records.

The final selection consists of 60 horizontal accelerograms for each combination of event type and soil class. In other words, 360 horizontal components are used for evaluating the η factors for a given deaggregation period T^*; the selected records for different T^* values are not identical as the target magnitude-distance criteria for the record selection depend on T^* (see Table 1). Figure 1 illustrates the magnitude-distance distribution of the selected records for soil classes C and D. Figure 2 shows the 5%-damped displacement spectra and the corresponding mean and standard deviation from the selected records based on T^* = 0.2 s.

DAMPING REDUCTION FACTORS

To investigate the correlation between the η factors and damping ratios in each bin and in the considered period range, we first compute the ratio between the obtained displacement amplitudes at damping levels ξ = 10%, 15%, 20%, 25%, and 30%, and those at ξ = 5% for each set of the selected records corresponding to each T^*. Figures 3 and 4 show the computed median η factors for the considered damping levels, event types, and soil classes. The choice of median as a representative statistical metric for the central tendency is motivated by the fact that the η factors can be approximated by the log-normal distribution. The effect of damping

ratio on η factors is clearly illustrated in these figures. As expected, smaller damping reduction factors are associated with higher damping levels. This is mainly due to the influence of damping ratio on the number of loading cycles, in a ground motion wave packet, required to reach a steady state for displacement (Bradley 2014). In comparison to low damping levels, the steady state is reached after fewer cycles at higher damping levels, resulting in considerably smaller spectral displacements, hence the smaller η factors. Figures 3 and 4 also show the dependency of computed η factors on the period T at which spectral displacements are determined.

We note that for all the three event types the significant period dependency of η factors at very short periods, i.e. shorter than approximately 0.15 s to 0.2 s is attributed to the facts that all the spectra at different damping levels approach a displacement amplitude of 0 towards $T = 0$ and gradually diverge as the period lengthens and the difference between the spectral displacements at various damping levels increases. In what follows we characterize the period dependency of the η factors beyond periods of 0.15 s to 0.2 s. The period dependency of the η factors is particularly noticeable for inslab records over the whole studied period range $0 \leq T \leq 3$ s.

Slight dependency on period is observed for crustal events as η increases moderately towards longer periods. The damping reduction factors of interface records show no significant period dependency, although minor influence of period can be observed at very short periods, i.e. $T \leq 0.5$ s, and long periods, i.e. 2.5 s $\leq T \leq 3$ s. These local decreases in the η factors are attributed to the existence of wave packets, in specific segments of ground motion records, having a narrow bandwidth of frequencies. This creates local spectral peaks in low damping spectra, i.e. $\xi = 5\%$, resulting in relatively smaller η factors at higher damping levels for which the wider bandwidth of frequencies produces smoother spectra (Bradley 2014). Damping reduction factors for inslab events are more evidently period dependent in comparison to the other two event types.

To obtain further insights about the event-type dependency of the η factors, the selected records are studied based on their frequency content and significant duration of ground motions. The significant duration is defined as the time interval of the Arias intensity between 5% and 95% (Trifunac and Brady 1975). The portion of each selected accelerogram corresponding to this duration measure is extracted. Rathje et al. (1998, 2004) suggested the mean period, T_{m}, as a robust measure of the frequency content of a ground motion, which can be computed using the following equation

$$T_{\mathrm{m}} = \frac{\sum_i C_i^2 / f_i}{\sum_i C_i} \tag{2}$$

where C_i represents the Fourier amplitude coefficients and f_i the discrete fast Fourier transform (FFT) frequencies between 0.25 and 20 Hz with Δf, the frequency intervals used in FFT computation, not greater than 0.05 Hz. The T_{m} values corresponding to each of the selected accelerograms are computed using Equation (2) and the results for the three event types are compared in Figure 5 for the two soil classes. Figure 5(a) shows that lower T_{m} values are associated with inslab events consistently, i.e. inslab events are of higher frequency content (attributed to high stress drop source parameters). This feature of inslab events is also mentioned by Chen et al. (2013). Considering a high-frequency record, a structure having a lower period of vibration undergoes more cycles in comparison to a structure having a longer

period and thus the effect of damping is more significant for the former (Naeim and Kircher 2001). This explains the smaller damping reduction factors at shorter periods for inslab events, which have richer high frequency content.

Figure 5(b) compares the duration of the selected records based on their event types. As expected, records from the selected interface events have considerably longer durations than those of the crustal and inslab events, due to the inclusion of very large events, i.e. **M**9 2011 Tohoku event. Bommer and Mendis (2005) and Zhou et al. (2014) reported a decrease in damping reduction factors with an increase in duration of records. The obtained damping reduction factors for interface events are smaller than those from other events and thus are in accordance with the observations of Bommer and Mendis (2005) and Zhou et al. (2014). Based on a study of harmonic excitation of single-degree-of-freedom systems, Zhou et al. (2014) also reported that the maximum displacement reaches a plateau and does not increase further when the system is subjected to a higher number of cycles, resulting in almost constant damping reduction factors at each damping level. The near-constant damping reduction factors for interface events that we obtain are in accord with these previous studies, and point to the importance of duration effects on damping when considering the engineering implications of great subduction earthquakes.

Figures 3 and 4 also compare the η factors from sets of records corresponding to each T^* at which PSHA is conducted. It is seen that the damping reduction factors for inslab and interface records are not influenced by the selected T^*. This is expected for interface events as the deaggregation results shown in Table 1 suggest that the same set of records is selected irrespective of the selected T^*. Moderate differences are observed for crustal events as a result of changes in T^*. Such differences are more noticeable at periods T approximately between 1 s and 1.7 s, where η factors from sets of records corresponding to $T^* \geq 1$ s demonstrate a less T^*-dependent behavior. Figure 5 also reveals a negligible effect of T^* on the general trends in frequency content and duration of the selected records. The minor changes in the scenarios, i.e. mean **M** and mean R_{rup}, for crustal and inslab events (Table 1) lead to the majority of the selected records for each T^* being similar, which explains the minor or even negligible effect of T^* on the η factors and the trends in the frequency content and duration of the selected records.

A comparison of the results in terms of soil class (i.e. Figures 3 and 4) reveals that the two soil classes, i.e. soil classes C and D, present broadly similar η factors. The negligible differences between the deaggregation results for soil classes C and D are the reason for such observations. The minor effect of site conditions on η factors from shallow crustal earthquakes has previously been reported in the literature (e.g. Lin and Chang 2004; Rezaeian et al. 2014).

As previously mentioned and illustrated in Figures 3 and 4, the trends in the η factors are not significantly affected by the T^* considered. Therefore, we combined all the already selected records for different T^*s and computed the corresponding median η factors at each period T. The results are shown in Figures 3 and 4 alongside those previously discussed. It can be seen that, despite some differences between the η factors computed from the Median and those from the sets of records corresponding to individual T^* for crustal events, the Median η factors can satisfactorily represent the η factors for each event. Figure 6 clearly illustrates that the Median η factors follow the previously observed trends in the η factors specific to each event. Figure 6 also reiterates the moderate effect of soil class on Median η factors for each event type and ξ considered.

ASSESSMENT OF AVAILABLE FORMULATIONS OF DAMPING REDUCTION FACTORS

Figures 3 and 4 also compare the computed damping reduction factors of the selected crustal, inslab, and interface records to predictions of available equations from Newmark and Hall (1973, 1982) [NH1973, NH1982], Bommer et al. (2000) [BEW2000], Zhou et al. (2003) [ZWX2003], Lin and Chang (2004) [LC2004], Atkinson and Pierre (2004) [AP2004], and AASHTO (2010). The results clearly show that the majority of the available equations are not capable of predicting the computed damping reduction factors satisfactorily. The discrepancies are more evident for the η factors from inslab events, for which significant period-dependency is observed. The damping reduction factors provided by Atkinson and Pierre (2004), although they do not cover the entire period range of study, capture such period dependency and thus have acceptable agreement with those computed using crustal and inslab records, while disagreement is observed for interface events. The η factors predicted by Zhou et al. (2003) agree well with computed damping reduction factors from interface records, however, these predictions become less accurate as higher damping levels are considered. It is important to note that the available predictions are based on record datasets that do not necessarily share the same record characteristics as the ones studied herein. Therefore, it is not surprising that these equations do not satisfactorily represent the observed trends of η factors for all three event types; indeed, the anticipated discrepancy was the motivation for this investigation. Moreover, the comparisons in Figures 3 and 4 highlight the need for a model equation that accounts for the distinct features of crustal, inslab, and interface earthquakes characterizing seismic hazard in south-western BC.

PROPOSED DAMPING REDUCTION FACTORS

In this work, we develop new period-dependent equations to characterize the median damping reduction factors for the events studied. One important criterion to be satisfied by the developed equation is that its functional form can be adapted to match the computed displacements spectra of the three event types, i.e. crustal, inslab, and interface, with the least misfits possible. After several trials, the following equation is proposed to approximate the η factors:

$$\eta = 1 - (1 + a_1[-\ln \xi]^{a_2})(a_3 + T)^{a_4} \exp(a_5 T^{a_6}) \tag{3}$$

The coefficients in Equation (3) are determined through nonlinear regression analyses using the least squares approach. Based on the observed trends for the η factors illustrated in Figures 3 and 4, one set of coefficients a_1 to a_6 for the entire period range of interest was first determined for the three event types. The results revealed that at least two sets of regression coefficients corresponding to period intervals 0 s $\leq T <$ 1 s and 1 s $< T \leq$ 3 s, respectively, are required to obtain sufficiently accurate predictions for all event types. Using more sets of coefficients corresponding to intervals below 1 s enhances the predictions at the very short period range, but at the same time complicates the use of the equation. Therefore, a compromise is made by providing coefficients a_1 to a_6 for the two period ranges 0 s $\leq T <$ 1 s and 1 s $< T \leq$ 3 s in Tables 2 and 3 for crustal, inslab, and interface events corresponding to soil classes C and D, respectively. To provide a smoother transition between the two intervals, the η factor at 1 s is calculated as the average of the outcomes of predicting expressions at periods immediately before and after 1 s.

Table 2. Coefficients a_1 to a_6 for soil class C

Event Type	T*	Period range	a_1	a_2	a_3	a_4	a_5	a_6
Crustal	0.2 s	0.05 s ≤ T < 1 s	-0.3130	1.0543	1.0	-0.3679	-0.0051	-2.0
		1 s < T ≤ 3 s	-0.4274	0.7743	1.0	-0.0282	-0.0112	2.0
	0.5 s	0.05 s ≤ T < 1 s	-0.3005	1.0924	1.0	-0.3843	-0.0051	-2.0
		1 s < T ≤ 3 s	-0.3451	0.9703	1.0	-0.1756	-0.1151	-2.0
	1.0 s	0.05 s ≤ T < 1 s	-0.3005	1.0924	1.0	-0.3843	-0.0051	-0.25
		1 s < T ≤ 3 s	-0.2860	1.1422	0.0	-0.3001	-0.1555	-0.5
	2.0 s	0.05 s ≤ T < 1 s	-0.2259	1.3561	1.0	-0.0542	-0.2860	0.0
		1 s < T ≤ 3 s	-0.2983	1.1034	0.0	-0.2611	-0.1432	-0.5
	3.0 s	0.05 s ≤ T < 1 s	-0.2001	1.4696	1.0	-0.3712	-0.1329	-0.5
		1 s < T ≤ 3 s	-0.3173	1.0473	0.0	-0.2530	-0.1338	-0.5
	Median	0.05 s ≤ T < 1 s	-0.2830	1.1469	1.0	-0.4443	-0.0057	-2.0
		1 s < T ≤ 3 s	-0.3254	1.0243	0.0	-0.2016	-0.1691	-0.5
Inslab	0.2 s	0.05 s ≤ T < 1 s	-0.1668	1.6345	1.0	-0.7997	-0.0334	-1.0
		1 s < T ≤ 3 s	-0.4102	0.8122	1.0	-0.0692	-0.0551	2.0
	0.5 s	0.05 s ≤ T < 1 s	-0.1713	1.6101	1.0	-0.8125	-0.0440	-0.75
		1 s < T ≤ 3 s	-0.4261	0.7759	0.0	-0.0436	-0.0524	2.0
	1.0 s	0.05 s ≤ T < 1 s	-0.1930	1.4987	1.0	-0.8814	-0.0033	-2.0
		1 s < T ≤ 3 s	-0.2965	1.1118	0.0	-0.6207	-0.3099	-2.0
	2.0 s	0.05 s ≤ T < 1 s	-0.1582	1.6838	1.0	-0.8783	-0.0337	-1.0
		1 s < T ≤ 3 s	-0.3170	1.0496	0.0	-0.6126	-0.3211	-3.0
	3.0 s	0.05 s ≤ T < 1 s	-0.1582	1.6838	1.0	-0.8783	-0.0337	-1.0
		1 s < T ≤ 3 s	-0.3170	1.0496	0.0	-0.6126	-0.3211	-3.0
	Median	0.05 s ≤ T < 1 s	-0.1711	1.6111	1.0	-0.7974	-0.0311	-1.0
		1 s < T ≤ 3 s	-0.4119	0.8080	0.0	-0.1661	-0.0404	2.0
Interface	0.2 s	0.05 s ≤ T < 1 s	-0.1740	1.5927	1.0	-0.4994	-0.0558	-1.0
		1 s < T ≤ 3 s	-0.1837	1.5443	0.0	-0.2009	-0.3620	-1.0
	0.5 s	0.05 s ≤ T < 1 s	-0.1740	1.5927	1.0	-0.4994	-0.0558	-1.0
		1 s < T ≤ 3 s	-0.1894	1.5162	1.0	-0.2296	-0.2111	-2.0
	1.0 s	0.05 s ≤ T < 1 s	-0.1612	1.6640	1.0	-0.5255	-0.0592	-1.0
		1 s < T ≤ 3 s	-0.1880	1.5225	1.0	-0.2340	-0.2015	-2.0
	2.0 s	0.05 s ≤ T < 1 s	-0.1612	1.6640	1.0	-0.5255	-0.0592	-1.0
		1 s < T ≤ 3 s	-0.1880	1.5225	1.0	-0.2340	-0.2015	-2.0
	3.0 s	0.05 s ≤ T < 1 s	-0.1740	1.5927	1.0	-0.4994	-0.0558	-1.0
		1 s < T ≤ 3 s	-0.1894	1.5162	1.0	-0.2296	-0.2111	-2.0
	Median	0.05 s ≤ T < 1 s	-0.1695	1.6172	1.0	-0.5019	-0.0578	-1.0
		1 s < T ≤ 3 s	-0.1882	1.5221	1.0	-0.2347	-0.2033	-2.0

Table 3. Coefficients a_1 to a_6 for soil class D

Event Type	T*	Period range	a_1	a_2	a_3	a_4	a_5	a_6
Crustal	0.2 s	0.05 s ≤ T < 1 s	-0.2860	1.1355	1.0	-0.4608	-0.0184	-1.5
		1 s < T ≤ 3 s	-0.3978	0.8381	0.5	0.5850	-0.3221	1.0
	0.5 s	0.05 s ≤ T < 1 s	-0.4368	0.7441	0.0	-0.0717	-0.0056	-2.0
		1 s < T ≤ 3 s	-0.4324	0.7597	0.0	0.3082	-0.0572	2.0
	1.0 s	0.05 s ≤ T < 1 s	-0.2885	1.1276	0.0	0.1492	-0.3686	3.0
		1 s < T ≤ 3 s	-0.2851	1.1477	0.0	0.3055	-0.2697	1.0
	2.0 s	0.05 s ≤ T < 1 s	-0.2305	1.3377	0.0	0.2708	-0.5437	3.0
		1 s < T ≤ 3 s	-0.3185	1.0434	3.0	-0.0732	-0.0136	3.0
	3.0 s	0.05 s ≤ T < 1 s	-0.1935	1.4988	0.0	0.2830	-0.4626	2.0
		1 s < T ≤ 3 s	-0.3087	1.0715	3.0	-0.0931	-0.0115	3.0
	Median	0.05 s ≤ T < 1 s	-0.3283	1.0076	1.0	-0.3143	-0.0058	-2.0
		1 s < T ≤ 3 s	-0.3482	0.9619	3.0	-0.0775	-0.0082	3.0
Inslab	0.2 s	0.05 s ≤ T < 1 s	-0.2206	1.3747	0.0	0.1755	-0.3741	2.0
		1 s < T ≤ 3 s	-0.3328	1.0053	0.0	-0.5173	-0.1317	-3.0
	0.5 s	0.05 s ≤ T < 1 s	-0.2206	1.3747	0.0	0.1755	-0.3741	2.0
		1 s < T ≤ 3 s	-0.3328	1.0053	0.0	-0.5173	-0.1317	-3.0
	1.0 s	0.05 s ≤ T < 1 s	-0.1710	1.6111	1.0	-0.5301	-0.0560	-1.0
		1 s < T ≤ 3 s	-0.3325	1.0063	0.0	-0.5041	-0.1159	-2.0
	2.0 s	0.05 s ≤ T < 1 s	-0.1882	1.5223	1.0	-0.5087	-0.0481	-1.0
		1 s < T ≤ 3 s	-0.3714	0.9045	0.0	-0.4691	-0.0332	-2.0
	3.0 s	0.05 s ≤ T < 1 s	-0.1882	1.5223	1.0	-0.5087	-0.0481	-1.0
		1 s < T ≤ 3 s	-0.3714	0.9045	0.0	-0.4691	-0.0332	-2.0
	Median	0.05 s ≤ T < 1 s	-0.2243	1.3594	0.0	0.1680	-0.3747	2.0
		1 s < T ≤ 3 s	-0.3597	0.9339	0.0	-0.4691	-0.0763	-3.0
Interface	0.2 s	0.05 s ≤ T < 1 s	-0.2089	1.4240	1.0	-0.4591	-0.0095	-2.0
		1 s < T ≤ 3 s	-0.1988	1.4716	1.0	-0.2868	-0.0886	-2.0
	0.5 s	0.05 s ≤ T < 1 s	-0.2089	1.4240	1.0	-0.4591	-0.0095	-2.0
		1 s < T ≤ 3 s	-0.1988	1.4716	1.0	-0.2868	-0.0886	-2.0
	1.0 s	0.05 s ≤ T < 1 s	-0.2204	1.3749	1.0	-0.4369	-0.0093	-2.0
		1 s < T ≤ 3 s	-0.2014	1.4600	1.0	-0.2950	-0.0893	-2.0
	2.0 s	0.05 s ≤ T < 1 s	-0.2204	1.3749	1.0	-0.4369	-0.0093	-2.0
		1 s < T ≤ 3 s	-0.2014	1.4600	1.0	-0.2950	-0.0893	-2.0
	3.0 s	0.05 s ≤ T < 1 s	-0.2204	1.3749	1.0	-0.4369	-0.0093	-2.0
		1 s < T ≤ 3 s	-0.2014	1.4600	1.0	-0.2950	-0.0893	-2.0
	Median	0.05 s ≤ T < 1 s	-0.2066	1.4343	1.0	-0.4756	-0.0097	-2.0
		1 s < T ≤ 3 s	-0.2048	1.4446	1.0	-0.2906	-0.0824	-2.0

Figures 7 and 8 compare the median η factors for 10%-, 20%-, and 30%-damped displacement spectra computed from sets of records corresponding to each T^* for the three considered event types and the two soil classes with the predicted η factors obtained using proposed Equation (3). Figures 7 and 8 show that there is generally a good agreement between the model predictions and the computed η factors for all the three event types. The percentages of misfit are discussed later. Slight discrepancies are observed for crustal events particularly at very short periods as illustrated in Figures 7 and 8. Such misfits are neglected to allow better predictions at longer periods.

The predictions of the proposed Equation (3) are then extended to the Median η factors and the results are compared to the computed ones in Figures 7 and 8. To predict the Median η factors, the corresponding coefficients a_1 to a_6 are provided in Tables 2 and 3. Figures 9 and 10 illustrate the standard deviations in logarithmic scale (St. Dev.) corresponding to the median η factors for soil classes C and D, respectively. The dispersion of the η factors increases as the damping level increases. However, it does not exceed 0.3 units for both soil classes. For crustal records, the observed differences in the dispersion of η factors about the mean are due to the larger variations of the selected records at each T^*. The selected inslab and interface records are quite similar for each T^* and thus the corresponding dispersion about the mean does not vary significantly with T^*.

For a more quantitative assessment of the performance of the model, the spectral displacements obtained using the proposed equation are compared to those given by the other available relationships described previously. The percentage of error corresponding to each expression of damping factor η in predicting computed spectral displacements $S_d(T,\xi)$ for damping ξ at period T is determined as

$$\text{Error (\%)} = \frac{\eta\, S_d(T, 5\%) - S_d(T, \xi)}{S_d(T, \xi)} \times 100 \tag{3}$$

The comparisons of the errors associated with the models of this study to those from the available literature are presented in Figures 11 to 16. These results show that the proposed models produce the least errors for the majority of cases over the entire period range considered The errors associated with a few combinations of T^* and ξ are relatively high which is due to the jagged shape of the corresponding median η factors as discussed earlier. Overall, it is concluded that the proposed equation can be effectively used to obtain damping reduction factors corresponding to crustal, inslab, and interface earthquakes characterizing seismic hazard in the city of Vancouver.

SUMMARY AND CONCLUSIONS

High-damping displacement spectra and corresponding damping reduction factors are important ingredients for the seismic design and analysis of structures equipped with energy dissipating and/or seismic isolation systems, as well as for displacement-based design methodologies. In this paper, damping reduction factors were evaluated for three main event types (i.e. crustal, inslab, and interface) contributing to the overall seismic hazard in south-western BC. For this purpose, a large dataset of 2302 records from the PEER-NGA, K-NET, KiK-net, and SK-net databases was first compiled. For each event type and soil type (i.e. NBCC soil classes C and D), 60 horizontal components were selected from the preliminary dataset based on seismic deaggregation results for Vancouver, the largest urban center in BC.

The median damping reduction factors of this final selection of records were then determined to investigate their characteristics.

We found that the damping reduction factors of inslab records depend significantly on period, while such dependency was shown to be less pronounced for crustal records and negligible for interface records. We also observed that the damping reduction factors are practically insensitive to the period at which PSHA is performed, although a slight influence of this parameter could be seen for crustal records. Minor differences were observed in the deaggregation results for soil classes C and D, hence approximately identical damping reduction factors were obtained for both cases. These observations were further investigated by studying the frequency content and significant duration of the selected records. The rich high frequency content of inslab records results in significant period dependency of the corresponding damping reduction factors due to the more significant influence of damping ratio at shorter periods for this event type. Furthermore, the considerably longer duration of interface records for very large events (i.e. the interval of Arias intensity between 5% and 95%) results in nearly-constant damping reduction factors; this is an important consideration in seismic design for the great Cascadia subduction event. We also illustrated that the Median damping reduction factors computed from all the selected records, regardless of the period at which PSHA is conducted, can be an acceptable representative of the median damping reduction factors for each event type. A comparison between the computed damping reduction factors obtained in this study and those estimated from previous equations motivated the need of developing new model equations, capable of more accurately modeling damping reduction factors for all three types of events that contribute to the seismic hazard of south-western BC. The spectral displacements obtained using the proposed equation were validated against computed spectral displacements of the selected records. We showed that the proposed predictions provide a satisfactory evaluation of damping reduction factors corresponding to crustal, inslab, and interface earthquakes.

ACKNOWLEDGEMENTS

The authors would like to acknowledge the financial support of the Natural Sciences and Engineering Research Council of Canada (NSERC) and the Canadian Seismic Research Network (CSRN). Strong ground-motion data were obtained from the PEER-NGA database (http://peer.berkeley.edu/nga/), the K-NET at www.k-net.bosai.go.jp, the KiK-net at www.kik.bosai.go.jp, and the SK-net at www.sknet.eri.u-tokyo.ac.jp.

REFERENCES

AASHTO, American Association of State Highway and Transportation Officials, 2010. *AASHTO LRFD Bridge Design Specifications*. Washington, D.C.

Adams, J., and Halchuk, S., 2003. Fourth generation seismic hazard maps of Canada: Values for over 650 Canadian localities intended for the 2005 National Building Code of Canada. Geological Survey of Canada Open File 4459.

Akkar, S., and Bommer, J. J., 2007. Prediction of elastic displacement response spectra in Europe and the Middle East. *Earthquake Engineering and Structural Dynamics* **36**, 1275-1301.

ASCE7-10, American Society of Civil Engineers, 2010. *ASCE7-10 Minimum design loads for buildings and other structures*. Reston, Virginia.

ATC, Applied Technology Council, 2010. *Modeling and Acceptance Criteria for Seismic Design and Analysis of Tall Buildings. ATC72-1*, Redwood City, CA.

Atkinson, G. M., and Boore, D. M., 1995. Ground-motion relations for eastern North America. *Bulletin of the Seismological Society of America*, **85**, 17-30.

Atkinson, G. M., and Pierre, J. R., 2004. Ground-motion response spectra in eastern North America for different critical damping values. *Seismological Research Letters* **75**, 541-545.

Atkinson, G. M., and Goda, K., 2011. Effects of seismicity models and new ground motion prediction equations on seismic hazard assessment for four Canadian cities. *Bulletin of the Seismological Society of America*, 101, 176-189.

Baker, J. W., and Cornell, C. A., 2006. Spectral shape, epsilon and record selection. Earthquake Engineering and Structural Dynamics, **35**, 1077-1095.

Berge-Thierry, C., Cotton, F., Scotti, O., Griot-Pommera. D. A., and Fukushima, Y., 2003. New empirical spectral attenuation laws for moderate European earthquakes. *Journal of Earthquake Engineering*, **7**, 193-222.

Bommer, J. J., Elnashai, A. S., Chlimintzas, G. O., and Lee, D., 1998. *Review and development of response spectra for displacement-based design*. ESEE Research Report No. 98-3, Imperial College London.

Bommer, J. J., Elnashai, A. S., and Weir, A. G., 2000. Compatible acceleration and displacement spectra for seismic design codes. *Proceedings of the 12th World Conference on Earthquake Engineering*, Auckland, New Zealand, Paper No. 0207.

Bommer , J., J., and Mendis, R., 2005. Scaling of spectral displacement ordinates with damping ratios. *Earthquake Engineering and Structural Dynamics*, **34**, 145-165.

Boore, D. M., Joyner, W. B., and Fumal, T. E., 1993. *Estimation of response spectra and peak accelerations from western North American earthquakes: an interim report*. US Geological Survey Open-File Report.

Bradley, B. A., 2014. The influence of source- and site-specific effects on response spectrum damping modification factors. *Earthquake Spectra*, doi: http://dx.doi.org/10.1193/070213EQS189M.

Cameron, W. I., and Green, R. A., 2007. Damping correction factors for horizontal ground-motion response spectra. *Bulletin of the Seismological Society of America*, **97**, 934-960.

Cardone, D., Dolce, M., and Rivelli, M. 2009. Evaluation of reduction factors for high-damping design response spectra. *Bulletin of Earthquake Engineering*, **7**, 273-291.

Cauzzi, C., and Faccioli, E., 2008. Broadband (0.05 to 20 s) prediction of displacement response spectra based on worldwide digital records. *Journal of Seismology*, **12**, 453-475.

CHBDC, Canadian Highway Bridge Design Code, Canadian Standards Association 2006. *CAN/CSA-S6-06 Standard*, Ontario.

Chen, Y., and Yu, Y., 2008. The development of attenuation relations in the rock sites for periods (T = 0.04 ~ 10 s, ξ = 0.005, 0.02, 0.07, 0.1 & 0.2) based on NGA database. *Proceedings of Fourteenth World Conference on Earthquake Engineering*, Beijing, China, Paper No. 03-02-0029.

Chen, K. H., Kennett, B. L. N., and Furumura, T., 2013. High-frequency waves guided by the subducted plates underneath Taiwan and their association with seismic intensity anomalies. *Journal of Geophysical Research: Solid Earth*, **118**, 1-16.

EC8, European Committee for Standardization, 2004. *Eurocode 8: Design of Structures for Earthquake Resistance - Part1: General Rules, Seismic Actions and Rules for Buildings. EN 1998-1, CEN*, Brussels, Belgium.

Goda, K., and Atkinson, G. M., 2009. Probabilistic characterization of spatially correlated response spectra for earthquakes in Japan. *Bulletin of the Seismological Society of America*, **99**, 3003-3020.

Goda, K., and Atkinson, G. M., 2010. Intraevent spatial correlation of ground-motion parameters using SK-net data. *Bulletin of the Seismological Society of America*, **100**, 3055-3067.

Goda, K., and Atkinson, G. M., 2011. Seismic performance of wood-frame houses in south-western British Columbia. *Earthquake Engineering and Structural Dynamics*, **40**, 903-924.

Hong, H. P., and Goda, K., 2006. A comparison of seismic-hazard and risk deaggregation. *Bulletin of the Seismological Society of America*, **96**, 2021-2039.

Jayaram, N., Baker, J. W., Okano, H., Ishida, H., McCann, M. W., and Mihara, Y., 2011. Correlation of response spectral values in Japanese ground motions. *Earthquakes and Structures*, **2**, 357-376.

Lin, Y. Y., and Chang, K. C., 2004. Effects of site classes on damping reduction factors. *Journal of Structural Engineering*, **130**, 1667-1675.

Naiem, F., and Kircher, C. A., 2001. On damping adjustment factors for earthquake response spectra. The *Structural Design of Tall Buildings*, **10**, 361-369.

NBCC, 2010. National Building Code of Canada, Associate Committee on the National Building Code, National Research Council of Canada, Ottawa, ON.

Newmark, N. M., and Hall, W. J., 1973. *Seismic design criteria for nuclear reactor facilities*. Report No. 46, Building Practices for Disaster Mitigation, National Bureau of Standards, US Department of Commerce.

Newmark, N. M., and Hall, W. J., 1982. *Earthquake spectra and design*. Earthquake Engineering Research Institute, Oakland, CA.

Priestley, M. J. N., and Kowalsky, M. J., 2000. Direct displacement-based seismic design of concrete buildings. *Bulletin of the New Zealand National Society for Earthquake Engineering*, **33**, 421-444.

Pina, F. E., 2010. *Methodology for the seismic risk assessment of low-rise school buildings in British Columbia*. Ph.D. Thesis, The University of British Columbia, Vancouver, BC.

Priestley, M. J. N., Calvi, G. M., and Kowalsky, M. J., 2007. *Displacement-based seismic design of structures*. IUSS Press, Pavia, Italy.

Rathje, E. M., Abrahamson, N. A., and Bray, J. D., 1998. Simplified frequency content estimates of earthquake ground motions. *Journal of Geotechnical and Geoenvironmental Engineering*, **124**, 150-159**.**

Rathje, E. M., Faraj, F., Russell, S., and Bray, J. D., 2004. Empirical relationships for frequency content parameters of earthquake ground motions. *Earthquake Spectra*, **20**, 119-144.

Rezaeian, S., Bozorgnia, Y., Idriss, I. M., Campbell, K. W., Abrahamson, M., and Silva, W. J., 2014. Damping scaling factors for elastic response spectra for shallow crustal earthquakes in active tectonic regions: "Average" horizontal component. *Earthquake Spectra*, **30**, 939-963.

Tehrani, P., Goda, K., Mitchell, D., Atkinson, G. M., and Chouinard, L. E., 2014. Effects of different record selection methods on the transverse seismic response of a bridge in south western British Columbia. *Journal of Earthquake Engineering*, **18**, 611-636.

Trifunac, M. D., and Brady, A. G., 1975. A study on the duration of strong earthquake ground motion. *Bulletin of the Seismological Society of America*, **65**, 581-626.

UBC-97, Uniform Building Code, International Code Council 1997. *Uniform building code*. UBC-97, Whittier, CA.

Zhou, F., Wenguang, L., and Xu, Z., 2003. State of the art on applications, R & D and design rules for seismic isolation in China. *Proceedings of the 8th World Seminar on Seismic Isolation, Energy Dissipation and Active Vibration Control of Structures*, Yerevan, Armenia.

Zhou, J., Tang, K., Wang, H., and Fang, X., 2014. Influence of ground motion duration on damping reduction factor. *Journal of Earthquake Engineering*, DOI: 10.1080/13632469.2014.908152

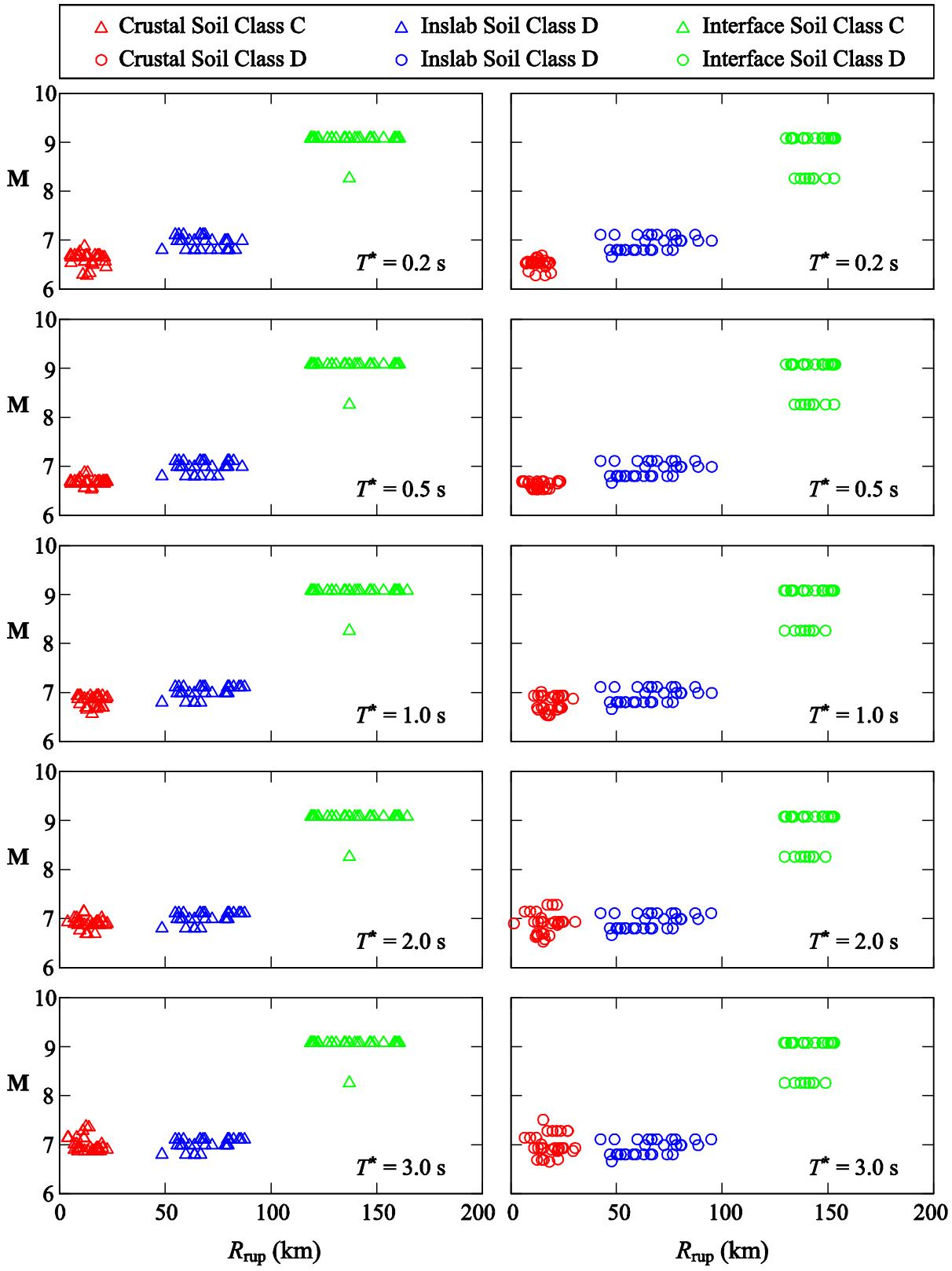

Figure 1. Magnitude-distance distribution of the selected records for soil classes C and D at different periods T^*.

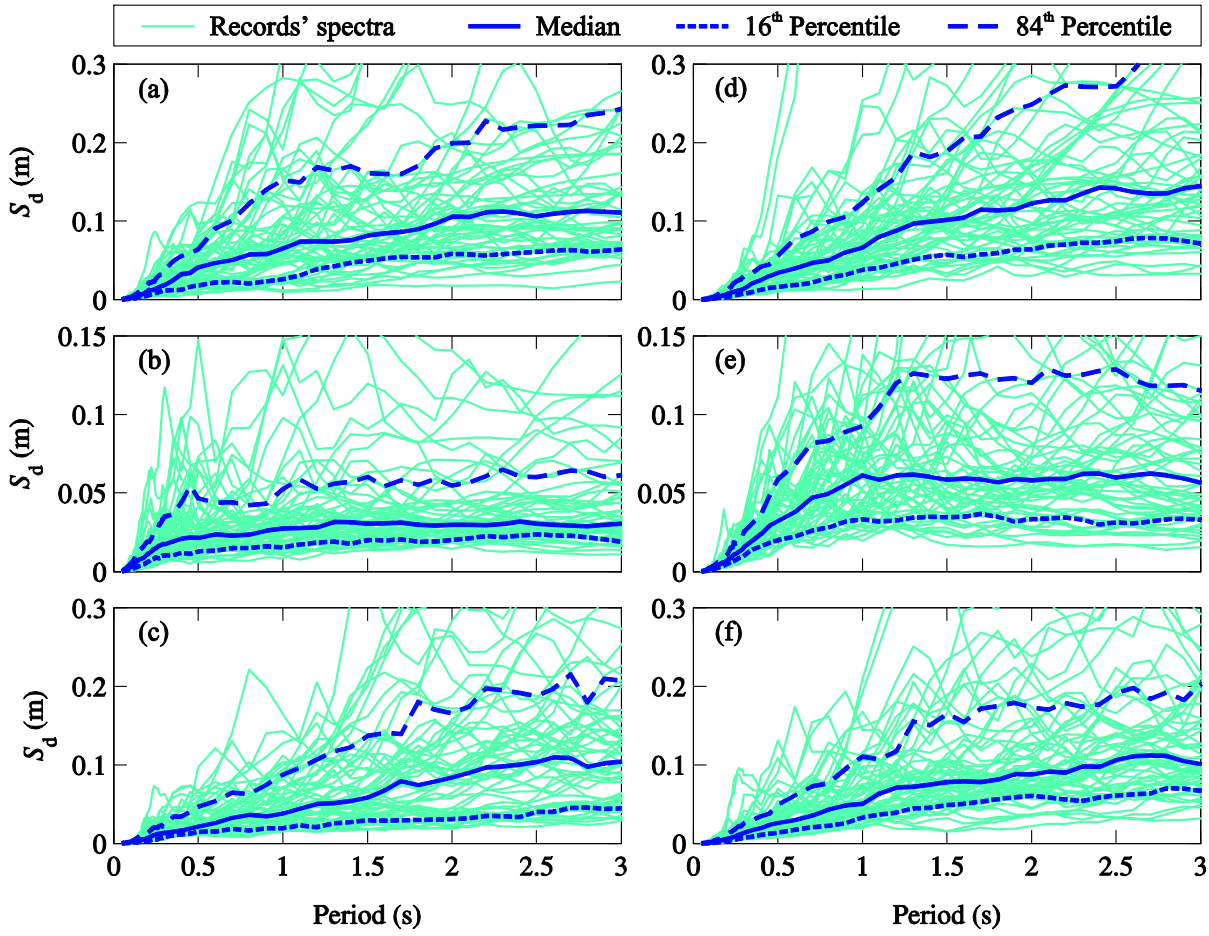

Figure 2. Selected records and corresponding medians of 5%-damped spectral displacements and 16th and 84th percentiles at T^* = 0.2 s: (a) and (d) Crustal events; (b) and (e) Inslab events, and (c) and (f) Interface events; (a) to (c) Soil class C and (d) to (f) Soil class D.

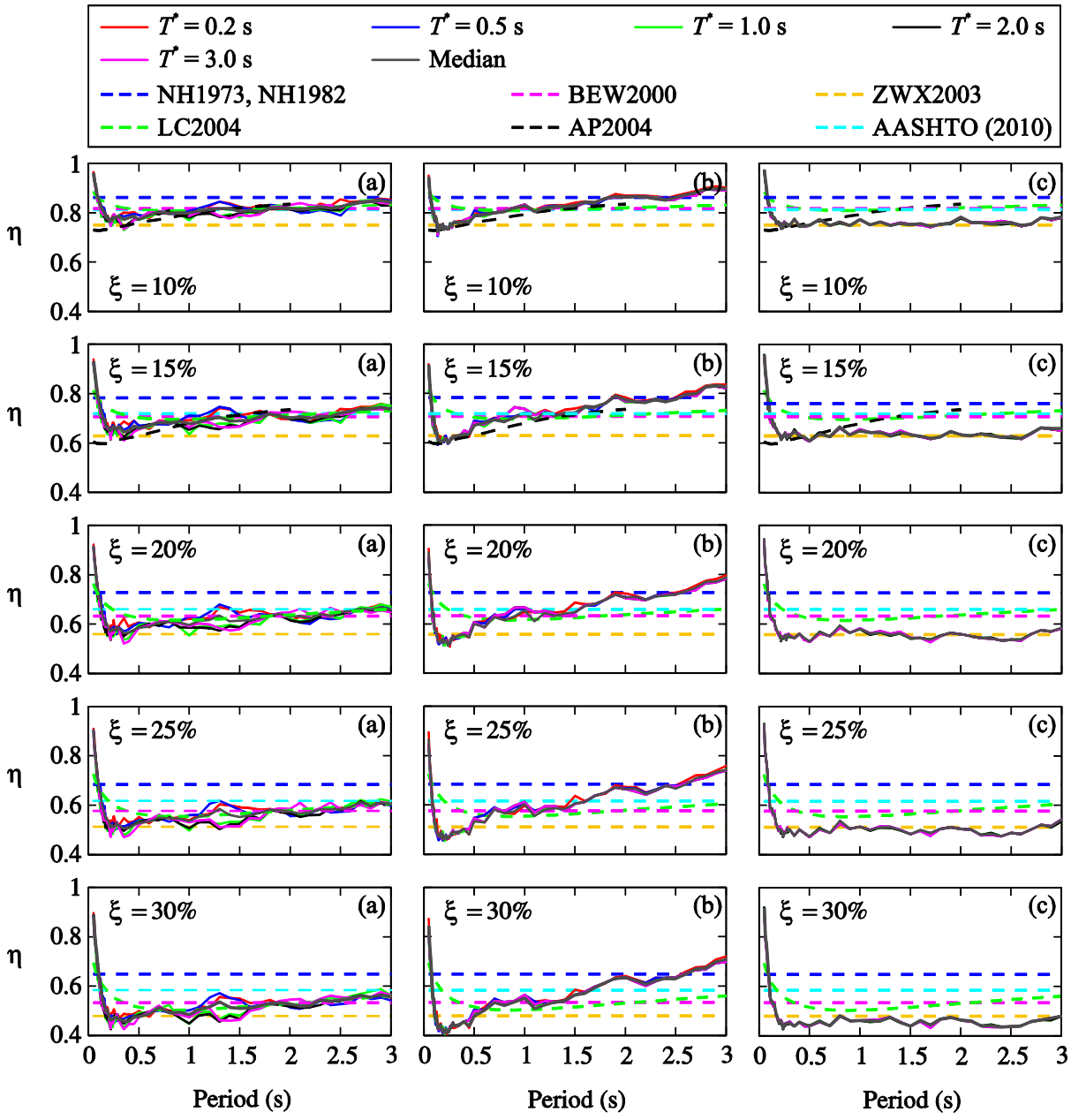

Figure 3. Damping reduction factors computed from the displacement spectra of the studied (a) Crustal, (b) Inslab and (c) Interface records for soil class C and predictions of some available equations.

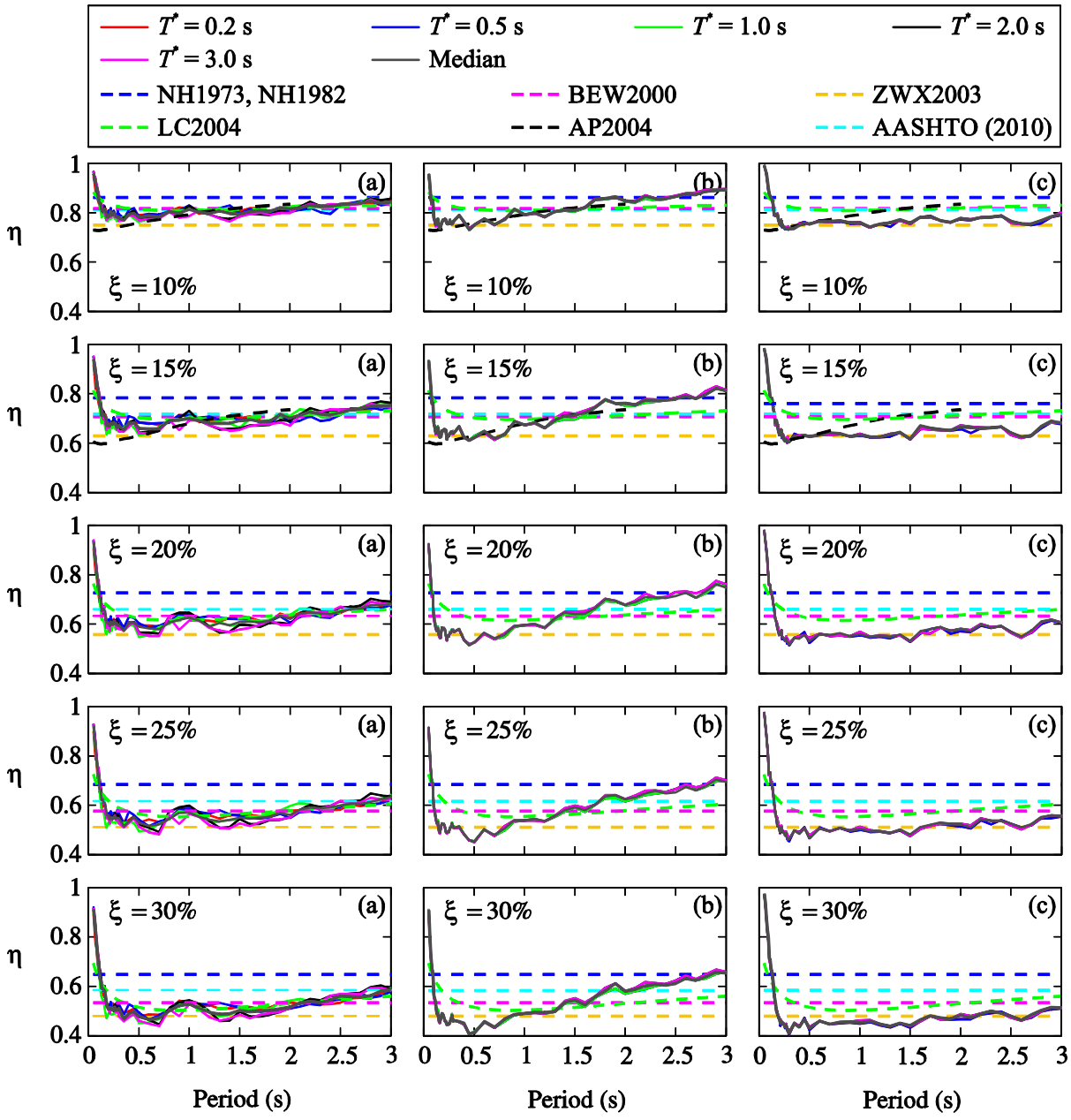

Figure 4. Damping reduction factors computed from the displacement spectra of the studied (a) Crustal, (b) Inslab and (c) Interface records for soil class D and predictions of some available equations.

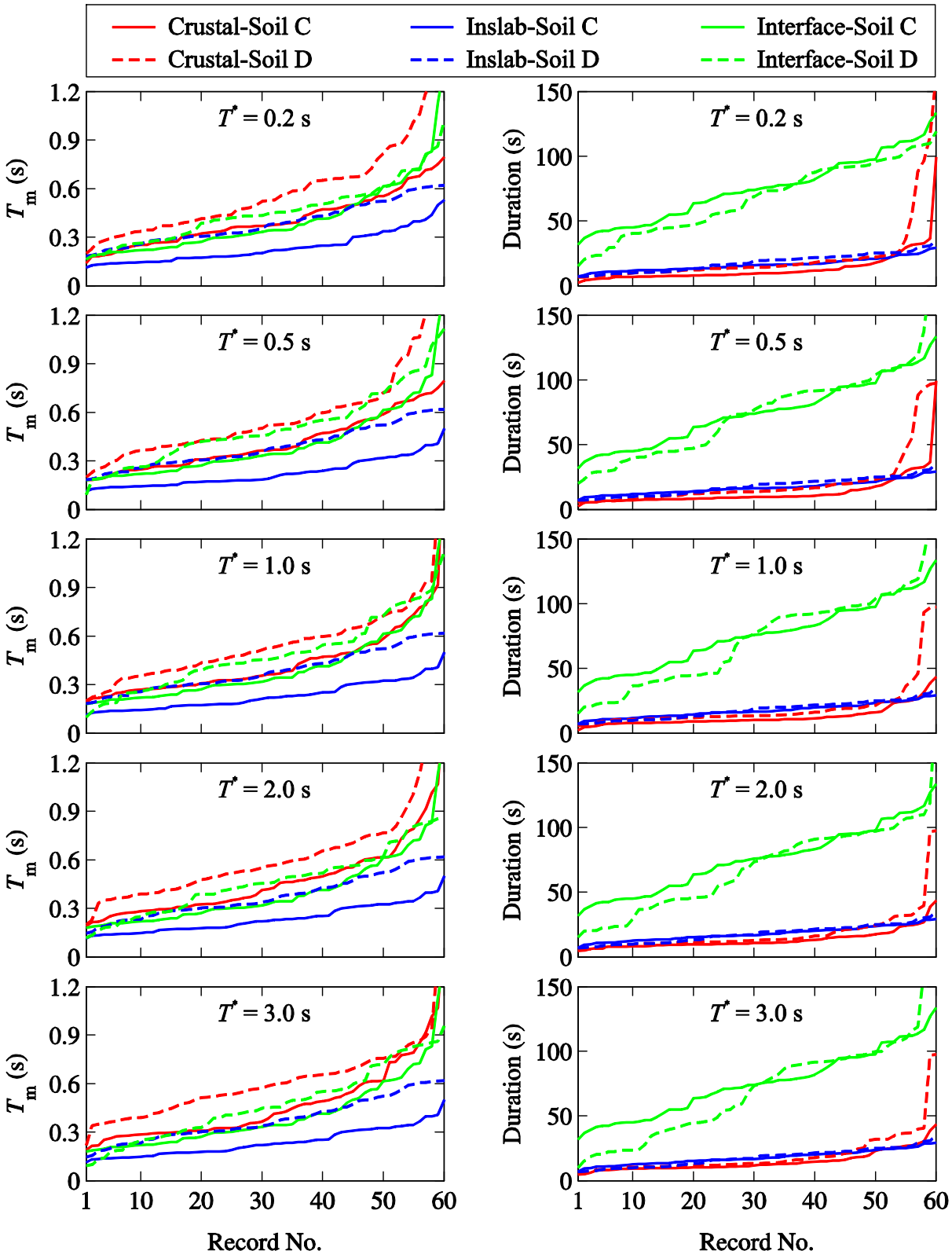

Figure 5. (a) Mean period and (b) duration for the 5%-95% Arias intensity interval of the selected records from the three event types at T^* = 0.2 s, 0.5 s, 1.0 s, 2.0 s and 3.0 s for soil classes C and D.

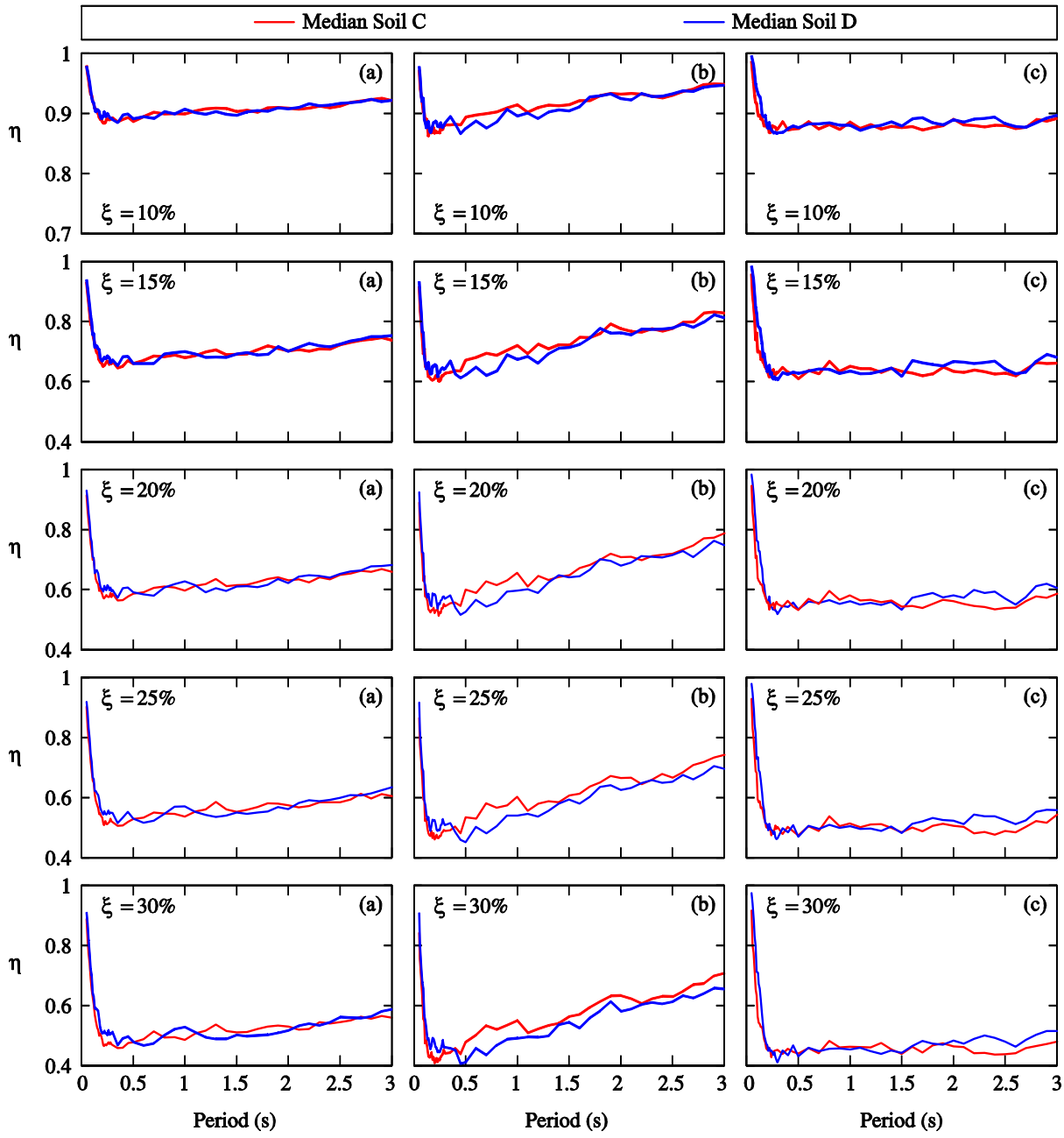

Figure 6. Median damping reduction factors computed by integrating all the sets of records corresponding to each T* for soil classes C and D: (a) Crustal, (b) Inslab and (c) Interface events.

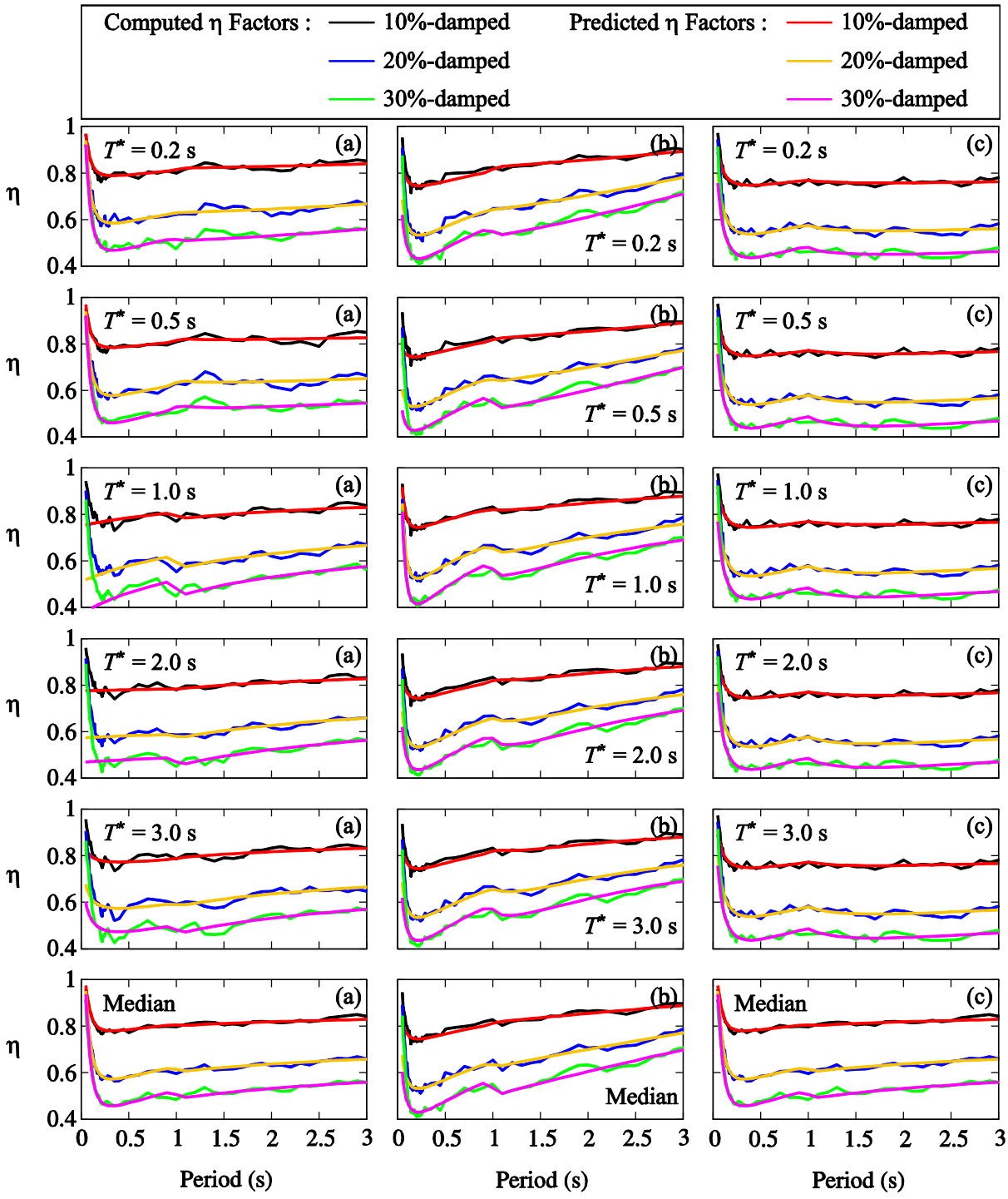

Figure 7. Comparison between the computed median damping reduction factors for (a) Crustal, (b) Inslab and (c) Interface events and the corresponding predictions at damping levels of 10%, 20% and 30% corresponding to soil class C.

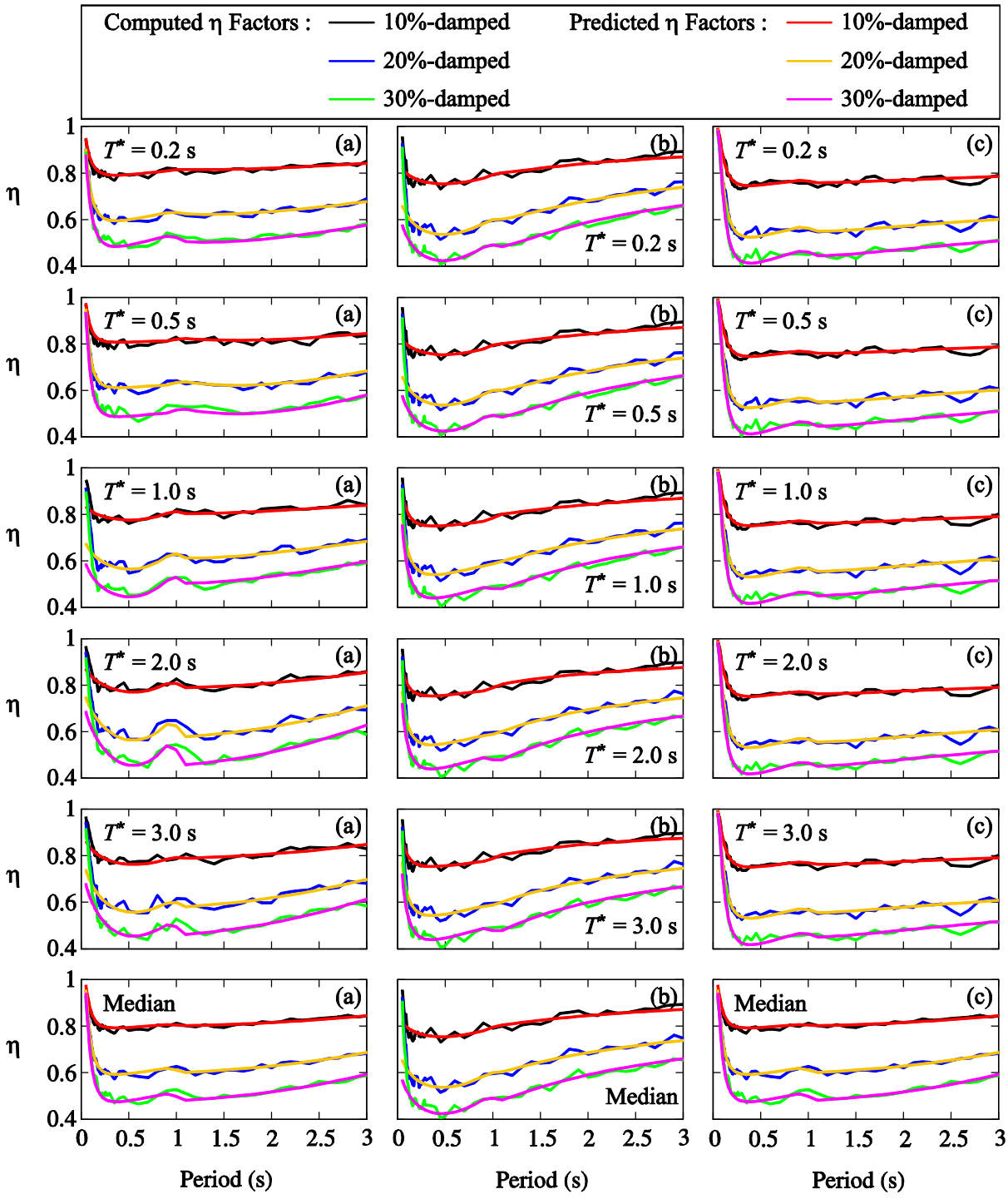

Figure 8. Comparison between the computed median damping reduction factors for (a) Crustal, (b) Inslab and (c) Interface events and the corresponding predictions at damping levels of 10%, 20% and 30% corresponding to soil class D.

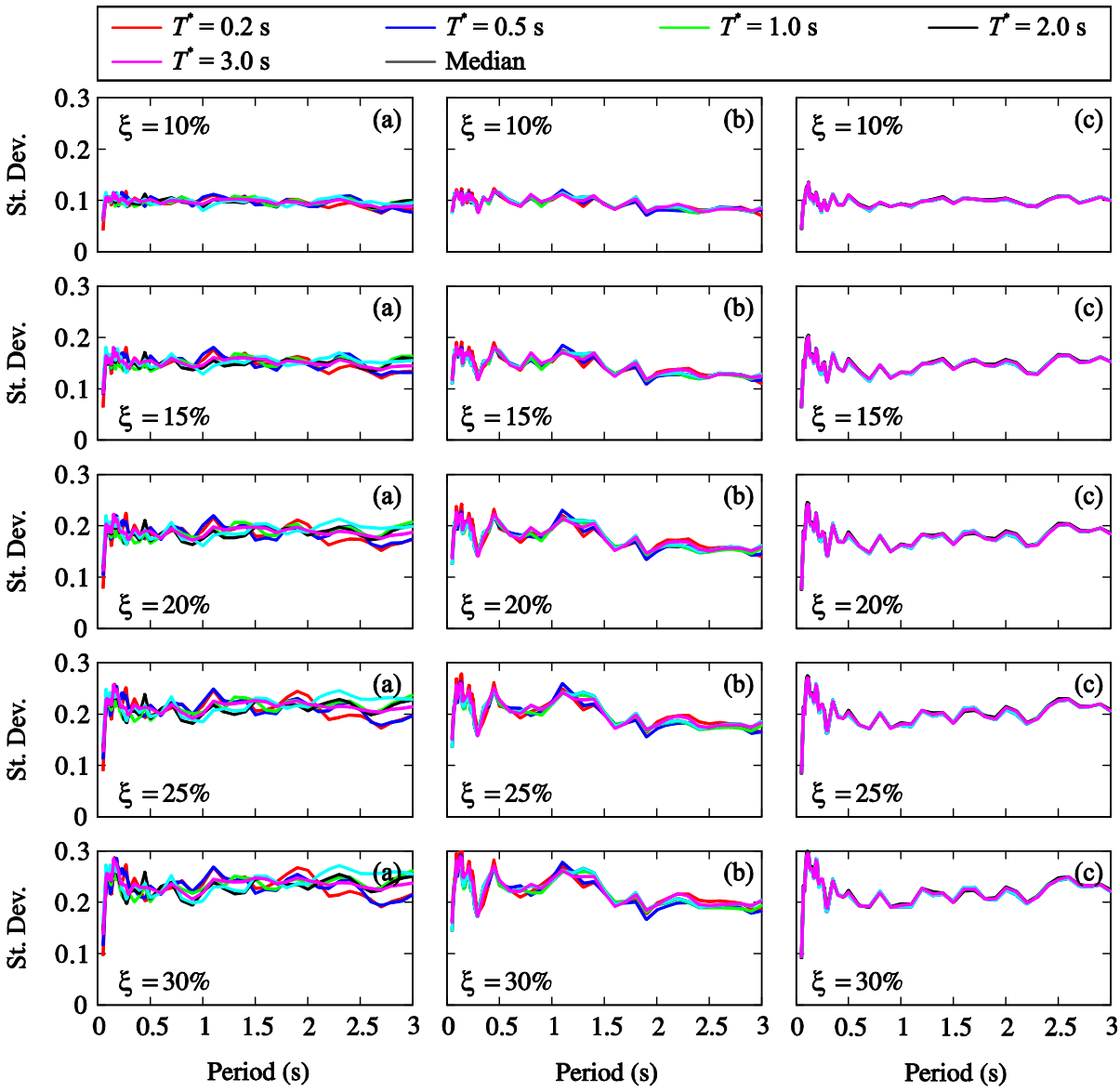

Figure 9. Standard deviations in logarithmic scale corresponding to median damping reduction factors for (a) Crustal, (b) Inslab and (c) Interface events corresponding to soil class C.

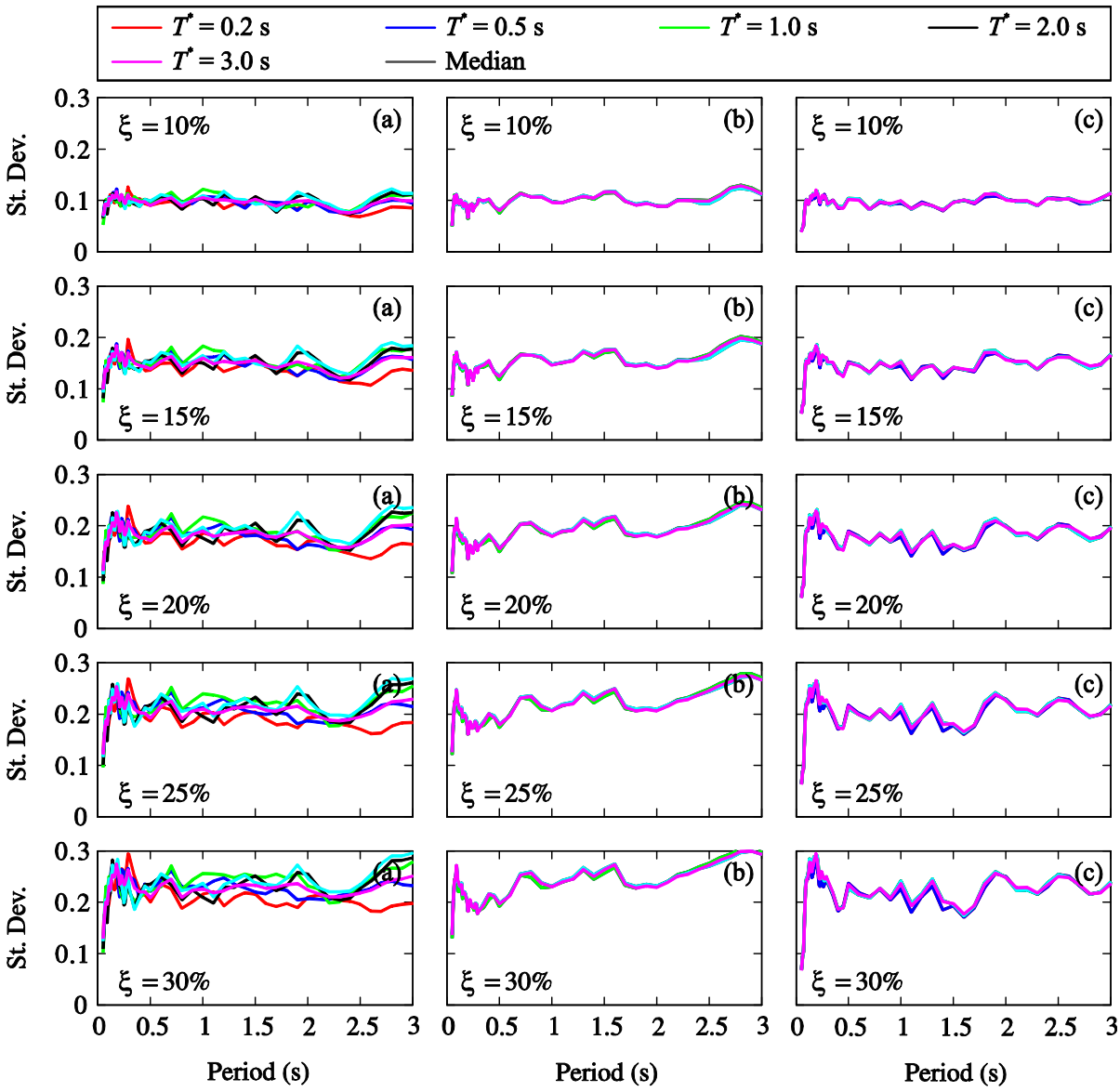

Figure 10. Standard deviations in logarithmic scale corresponding to median damping reduction factors for (a) Crustal, (b) Inslab and (c) Interface events corresponding to soil class D.

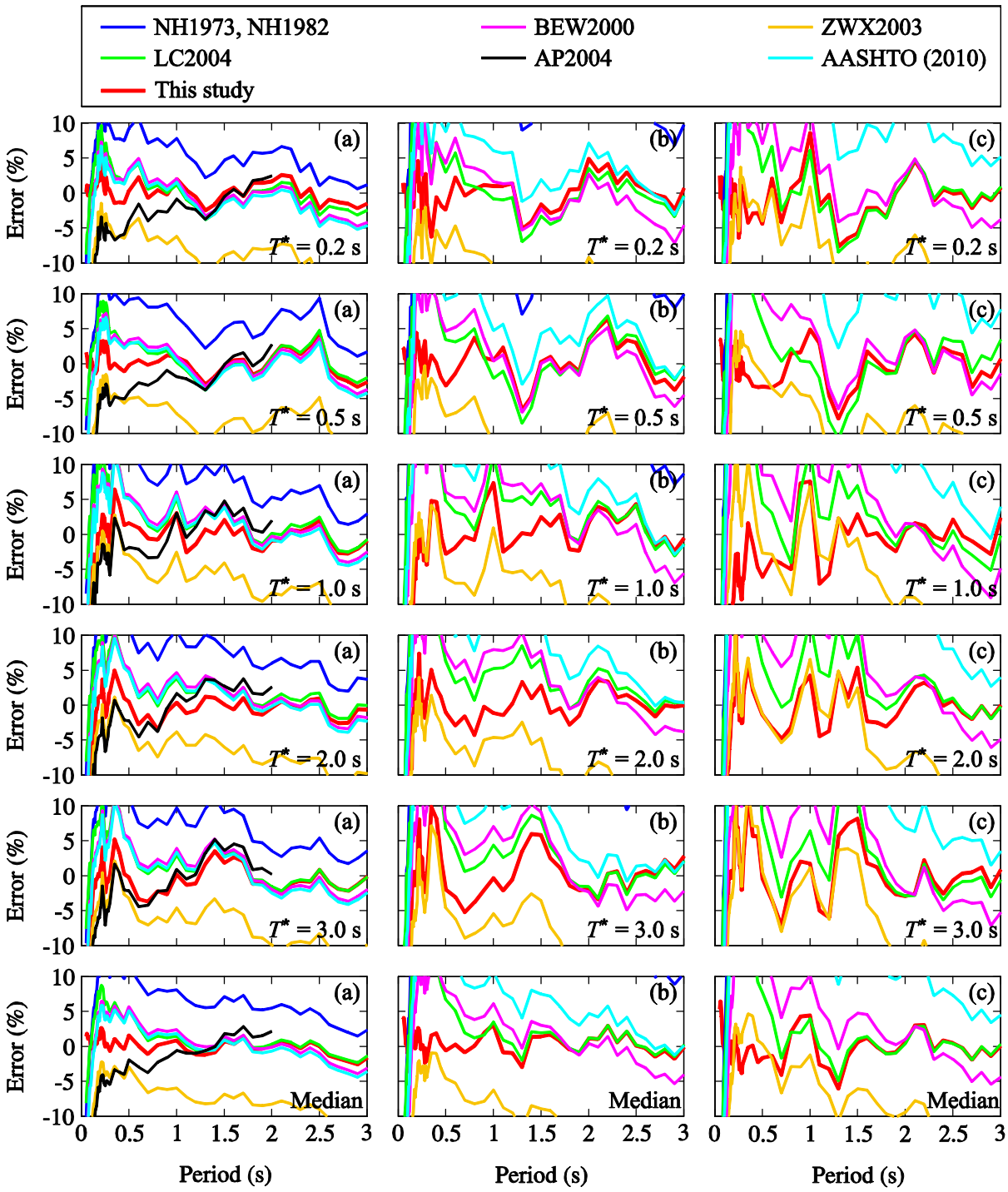

Figure 11. Percentages of error associated with different damping modification factor prediction equations available in the literature and the proposed equation at (a) 10%, (b) 20% and (c) 30% damping for crustal events corresponding to soil class C.

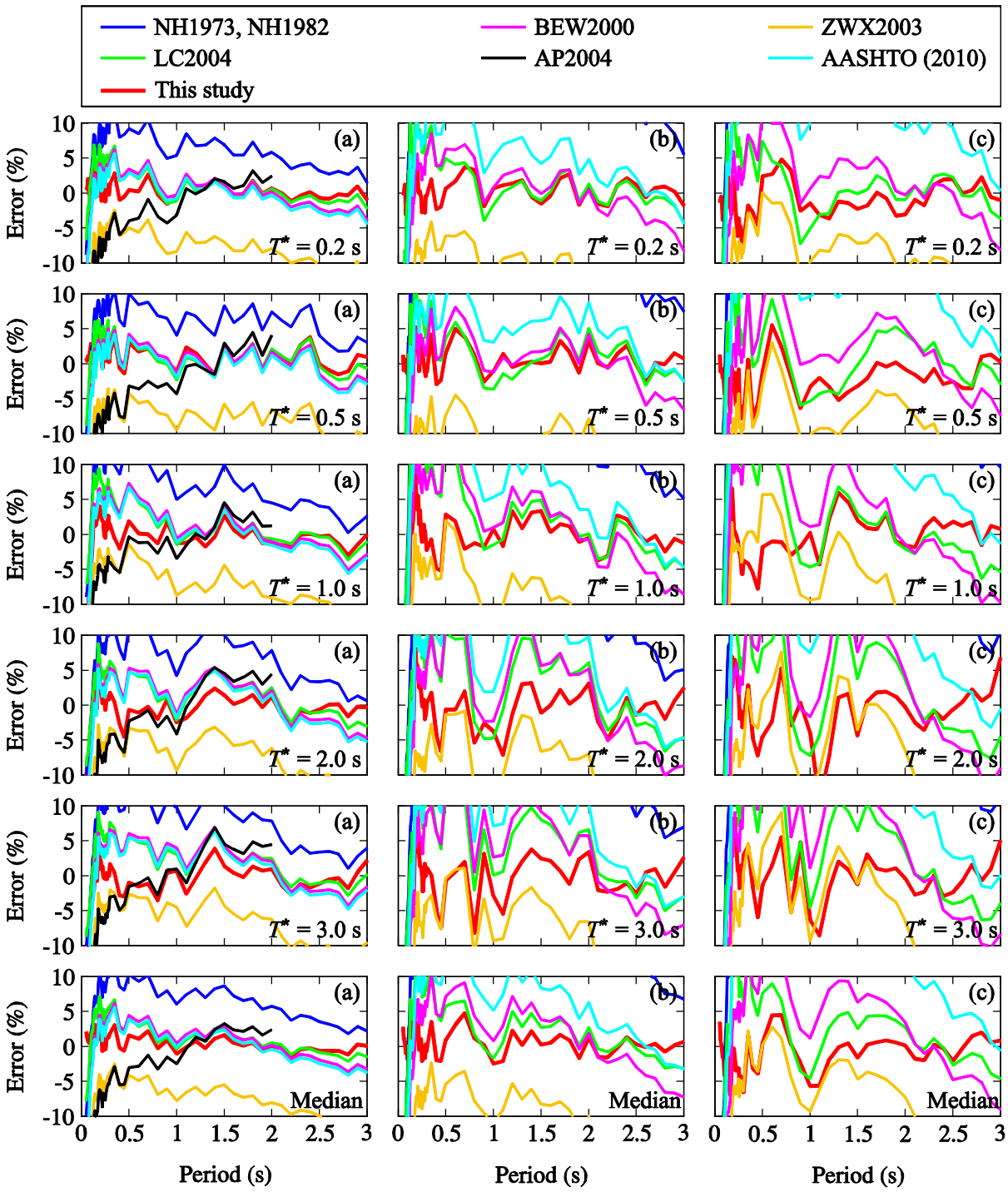

Figure 12. Percentages of error associated with different damping modification factor prediction equations available in the literature and the proposed equation at (a) 10%, (b) 20% and (c) 30% damping for crustal events corresponding to soil class D.

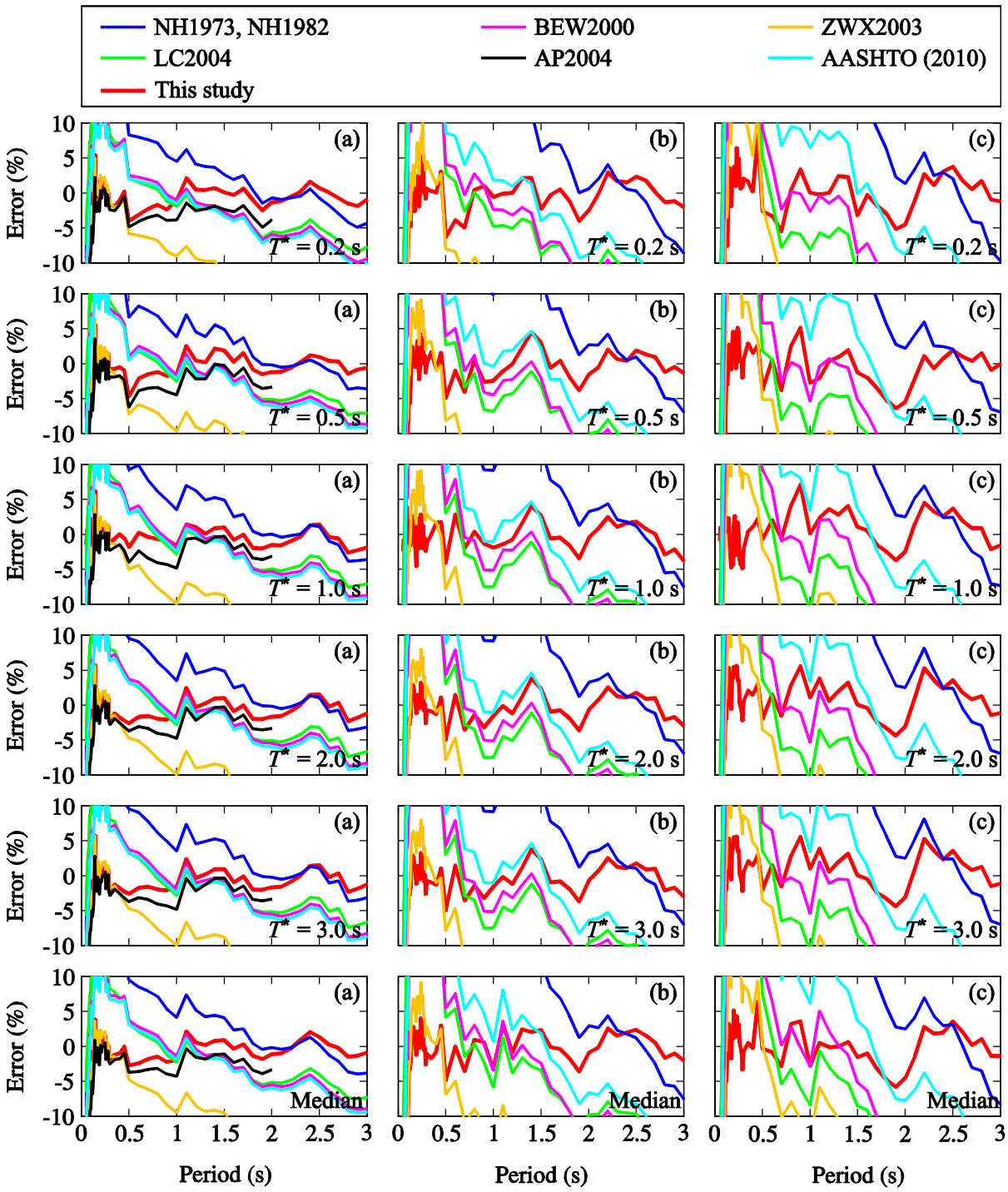

Figure 13. Percentages of error associated with different damping modification factor prediction equations available in the literature and the proposed equation at (a) 10%, (b) 20% and (c) 30% damping for inslab events corresponding to soil class C.

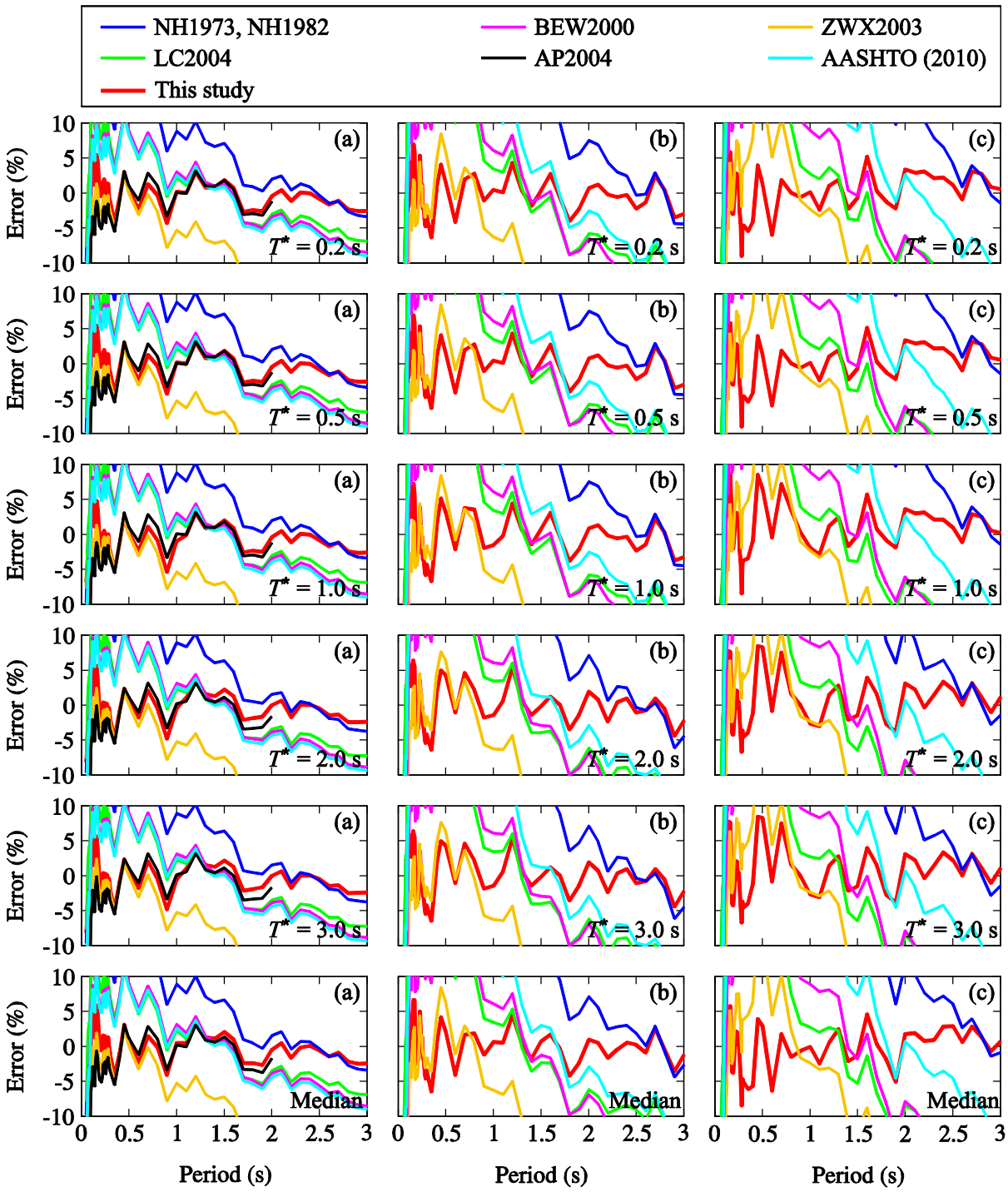

Figure 14. Percentages of error associated with different damping modification factor prediction equations available in the literature and the proposed equation at (a) 10%, (b) 20% and (c) 30% damping for inslab events corresponding to soil class D.

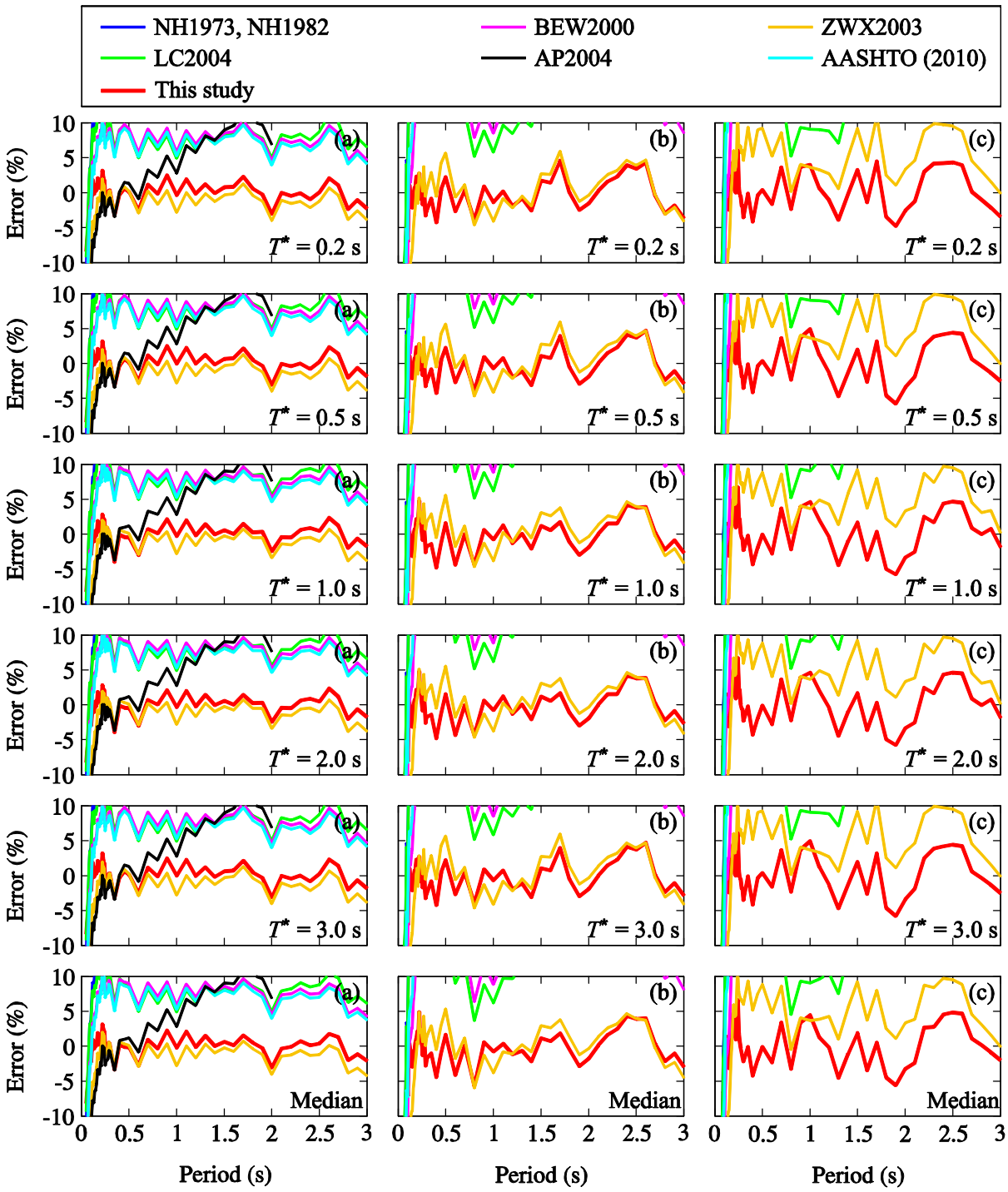

Figure 15. Percentages of error associated with different damping modification factor prediction equations available in the literature and the proposed equation at (a) 10%, (b) 20% and (c) 30% damping for interface events corresponding to soil class C.

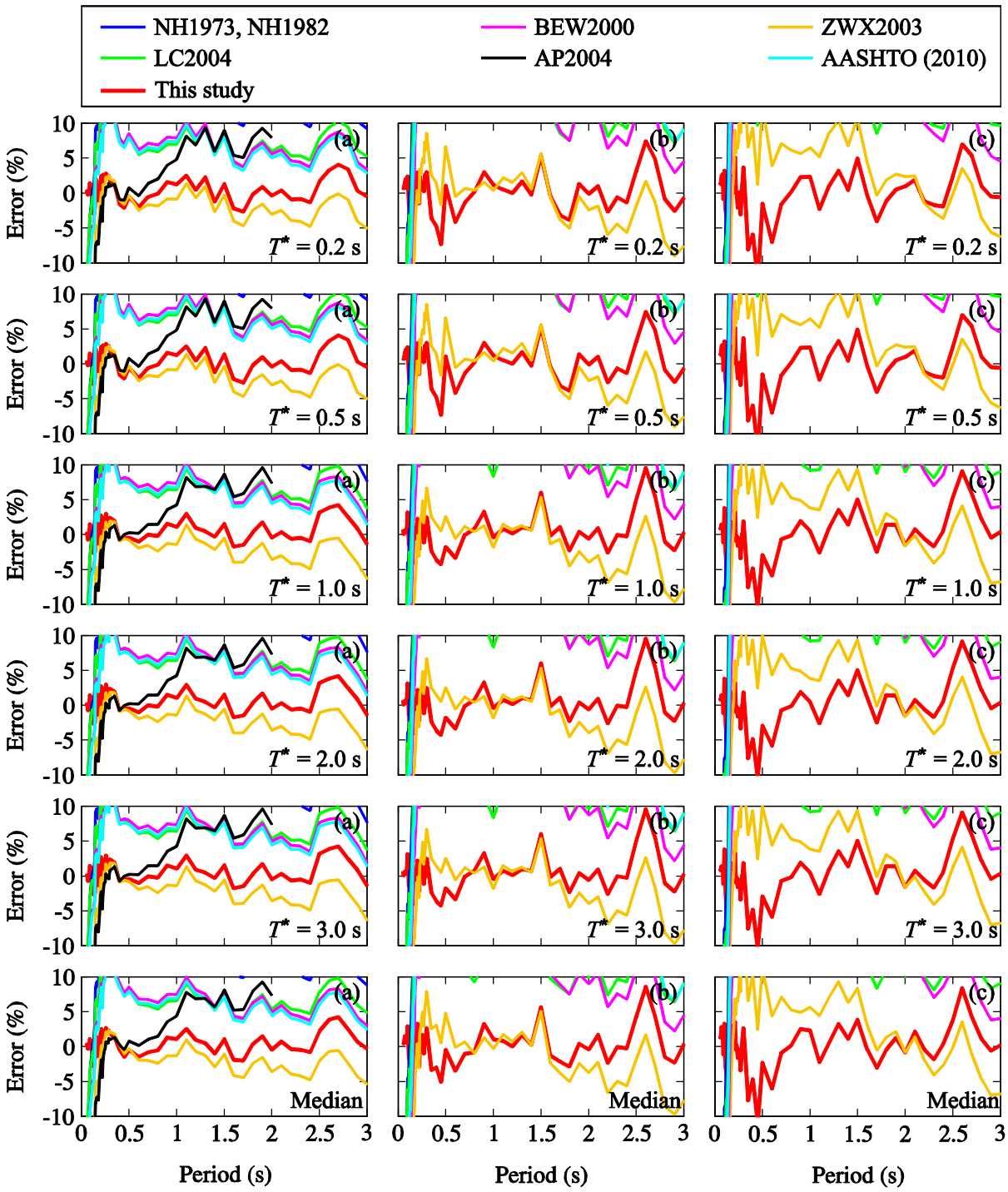

Figure 16. Percentages of error associated with different damping modification factor prediction equations available in the literature and the proposed equation at (a) 10%, (b) 20% and (c) 30% damping for interface events corresponding to soil class D.